Available online at www.sciencedirect.com
ScienceDirect
Geomorphology 88 (2007) 329–351
GEOMORPHOLOGY
www.elsevier.com/locate/geomorph

Sensitivity analysis of pediment development through numerical simulation and selected geospatial query

Mark W. Strudley *, A. Brad Murray

Division of Earth and Ocean Sciences, Nicholas School of the Environment and Earth Science, Center for Nonlinear and Complex Systems, Duke University, USA

Received 3 October 2006; received in revised form 29 November 2006; accepted 7 December 2006
Available online 23 December 2006

Abstract

Dozens of references recognizing pediment landforms in widely varying lithologic, climatic, and tectonic settings suggest a ubiquity in pediment forming processes on mountain piedmonts worldwide. Previous modeling work illustrates the development of a unique range in arid/semiarid piedmont slope (<0.2 or 11.3°) and regolith thickness (2–4 m) that defines pediments, despite varying the initial conditions and domain characteristics (initial regolith thickness, slope, distance from basin to crest, topographic perturbations, and boundary conditions) and process rates (fluvial sediment transport efficiency and weathering rates). This paper expands upon the sensitivity analysis through numerical simulation of pediment development in the presence of spatially varying rock type, various base level histories, various styles of sediment transport, and various rainfall rates to determine how pediment development might be restricted in certain environments. This work suggests that in landscapes characterized by soil and vegetation types that favor incisive fluvial sediment transport styles coupled with incisive base level conditions, pediment development will be disrupted by the roughening of sediment mantled surfaces, thereby creating spatial variability in topography, regolith thickness, and bedrock weathering rates. Base level incision rates that exceed the integrated sediment flux along a hillslope derived from upslope weathering and sediment transport on the order of 10^{-3} m y^{-1} restrict pediment development by fostering piedmont incision and/or wholesale removal (stripping) of regolith mantles prior to footslope pediment development. Simulations illustrate an insensitivity to alternating layers of sandstone and shale 3–15 m thick oriented in various geometric configurations (vertical, horizontal, and dip-slope) and generating different regolith hydrologic properties and exhibiting weathering rate variations up to 3-fold. Higher fluxes and residence times of subsurface groundwater in more humid environments, as well as dissolution-type weathering, lead to a thickening of regolith mantles on erosional piedmonts on the order of 10^1 m and an elimination of pediment morphology. An initial test of the model sensitivity analysis in arid/semiarid environments, for which field reconnaissance and detailed geomorphic mapping indicate the presence of pediments controlled by climatic conditions (soil hydrologic properties, vegetation characteristics, and bedrock weathering style) that are known and constant, supports our modeling results that pediments are more prevalent in hydrologically-open basins.

Keywords: Pediments; Tors; Weathering; Sediment transport; Arid landforms; Landscape evolution modeling

1. Introduction

The recognition and description of pediments, or smooth, extensive (on the order of km^2; hereafter

* Corresponding author. Current address: USDA-ARS, Agricultural Systems Research Unit, 2150-D Centre Avenue, Fort Collins, CO, 80526, USA. Tel.: +1 970 492 7323; fax: +1 970 492 7310.
E-mail address: mark.strudley@ars.usda.gov (M.W. Strudley).

0169-555X/$ - see front matter © 2006 Elsevier B.V. All rights reserved.
doi:10.1016/j.geomorph.2006.12.008

written as **O** (km^2)), gently sloping (0–10°) bedrock surfaces covered by a thin (**O** (m)) veneer of regolith, has driven a century-old debate regarding the nature of landscape evolution in mountainous terrain. Geologists typically regard pediments as arid landforms developed in granitic rocks, but their identification and description in a diverse range of climatic and lithologic environments has prompted some geomorphologists to consider pedimentation a diagnostic process governing landform development at the foot of both growing and decaying mountains worldwide (King, 1953; Whitaker, 1979). The voluminous literature on pediment landforms describes these features in a variety of lithologic environments, including quintessential felsic intrusive rocks (Sharp, 1957; Eggler et al., 1969; Oberlander, 1974; Twidale, 1981; Dohrenwend, 1994), metamorphic rocks (Eggler et al., 1969; Warnke, 1969; Twidale, 1981), volcanic rocks (Twidale, 1979; Whitaker, 1979; Dohrenwend, 1982; Wilshire and Reneau, 1992; Miller, 1995), and sedimentary rocks, including arkose (Warnke, 1969), breccias (Warnke, 1969), fanglomerate (Wilshire and Reneau, 1992), shale and siltstone (Morris, 1932; Rich, 1935; Miller, 1948; Knechtel, 1953; Schumm, 1962; Barth, 1976; Twidale, 1981), sandstone (Morris, 1932; Bryan and McCann, 1936; Knechtel, 1953; Barth, 1976), marls and limestones (Morris, 1932; Miller, 1948; Knechtel, 1953; Sharon, 1962; Barth, 1976; Twidale, 1979), argillaceous sedimentary rocks (Twidale, 1979), and other unspecified non-granitic rocks (Blackwelder, 1931; Bryan, 1932; King, 1949; Sharon, 1962; Cooke, 1970; Whitaker, 1979; Dohrenwend, 1982). Aridity does not seem to be a controlling factor in the development of pediments either, with pediments recognized in both arid (e.g., Berkey and Morris, 1932; Barth, 1976; Dohrenwend, 1994; Vincent and Sadah, 1996; Bourne and Twidale, 1998) and temperate/humid environments (Ruxton, 1958; Ruxton and Berry, 1961; Thomas, 1965; Fairbridge, 1977; Mills, 1983; Pavich, 1989; Thomas, 1989; Ballesteros and Martin, 2002; Beauvais et al., 2003; Clarke and Rendell, 2006). Despite previous modeling work (Strudley et al., 2006a) that suggests that pediment development does not depend on rock type, pediments are not present at the foot of every steep mountain front. Some mountainsides exhibit steep, corrugated slopes extending down to bedrock streams in v-shaped valleys, while others possess thick (10^1–10^2 m) sequences of soil and regolith grading into progressively thinner profiles and less weathered bedrock upslope. What climatic, tectonic, or geologic characteristics of a landscape, then, restrict pediments from developing?

Here we provide a test and sensitivity analysis through numerical simulation to determine how pediment development responds to the presence of spatially varying rock type, various base level histories, various styles of sediment transport, and various rainfall rates. These model tests build upon a fundamental understanding of pediment development elucidated by numerical simulations illustrating how smooth bedrock surfaces in granitic desert environments covered by a thin and nearly uniform blanket of regolith emerge spontaneously in a model coupling bedrock weathering and sediment transport by episodic streams (Strudley et al., 2006a). Fig. 1A illustrates how an equilibrium

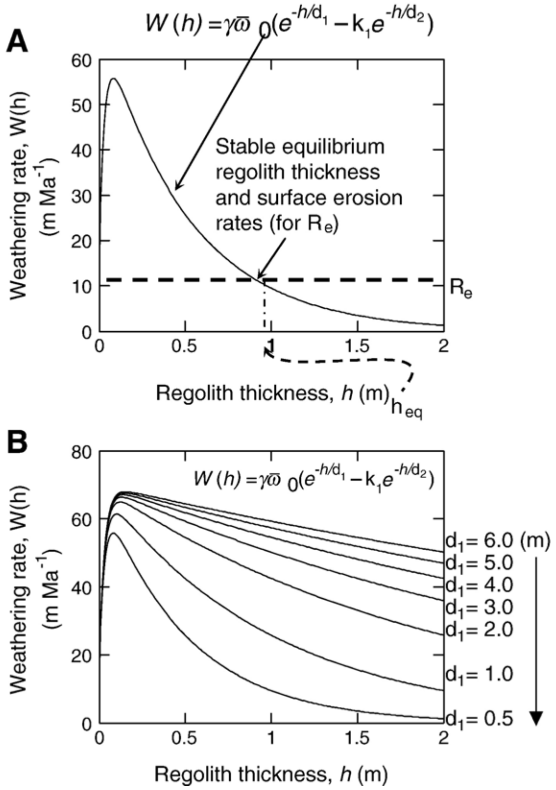

Fig. 1. Weathering rate, $W(h)$ (m Ma^{-1}), as a function of regolith thickness, h (m). (A) Relation between the function and the equilibrium regolith thickness (h_{eq}; described in text). Parameter values for weathering function described in text; bare-bedrock weathering rate is 14 m Ma^{-1}; d_1 = 0.5 m. Dashed line represents rate at which alluvial surface is lowering (erosion rates, labeled R_e in m Ma^{-1}). These erosion rates are determined by sediment flux divergence and boundary conditions. (B) Depiction of how alterations to d_1 (m) affect the bedrock-weathering rate as a function of regolith thickness. Bare-bedrock and maximum weathering rates remain fixed, while weathering rates accelerate at depth as d_1 increases. Values of d_1 above 0.5 m are chosen arbitrarily, and although not constrained by field measurements, elevated d_1 seeks to model general weathering behavior (see text).

regolith thickness develops in this model through the regulation of bedrock weathering by regolith thickness, which, in turn, reflects surface erosion rates. For example, when regolith thickness exceeds h_{eq}, bedrock-weathering rates are less than sediment surface erosion rates, and thus regolith profiles thin over time. This thinning causes bedrock weathering to accelerate, resulting in an equilibrium regolith thickness ($h \rightarrow h_{eq}$, from right in Fig. 1A). If regolith thickness falls below h_{eq}, regolith profiles thicken over time, causing bedrock-weathering rates to decrease; again, regolith thickness ultimately becomes stable ($h \rightarrow h_{eq}$, from left). In the numerical model developed by Strudley et al. (2006a), a smooth pediment surface with a uniform equilibrium regolith profile persists across the piedmont because the arid/semiarid climatic conditions assumed in our model—which constrain vegetation cover, storm characteristics, the style of bedrock weathering, and soil hydrologic properties—suppress fluvial incision. For example, lateral bank instability (Nichols et al., 2002) aided by sparsely vegetated, non-cohesive sediment in desert environments contributes to the smoothness of pediments, and can allow flows to bifurcate and effectively widen downslope so that water discharge per unit channel width increases less rapidly than in a corresponding channel of constant width. In addition, where convective, localized storms are important and infiltration rates are high (as in many desert environments), flow distances will be limited, reducing downstream flow concentration. Finally, the presence of non-cohesive soils promotes slope-driven, non-fluvial sediment transport driven by rainsplash, which tends to fill in rills and incipient channels in many arid/semiarid environments (Dunne and Aubry, 1986). If, however, we perform simulations in which our parameterizations of weathering and sediment transport processes (governed by climatic assumptions) change, will pedimentation remain a robust phenomenon at the foot of mountain slopes? For example, if more temperate/humid climatic conditions produce 1) intense or accelerated weathering leading to more cohesive sediments and restricted infiltration rates, 2) a more dense network of vegetation and roots, and/or 3) a shift from ephemeral fluvial processes to perennial flow, will piedmonts maintain the smooth surfaces and uniform regolith profiles necessary for pedimentation?

Our numerical modeling of pediment development also illustrates the importance of base level history (Strudley et al., 2006a). Simulations produce pediment landforms in hydrologically-open basins in which the downslope boundary is modeled as a fixed-elevation bounding stream system. Pediments in the model also evolve in hydrologically-closed basins in which the downslope boundary is modeled as an aggrading depositional basin (Strudley et al., 2006a), although in this case pediments primarily develop after an evolving mountain mass has weathered away, extending to the topographic crest. Will pedimentation persist, however, in the presence of tectonic and climatic conditions that foster base level incision?

We hypothesize that in landscapes characterized by soil and vegetation characteristics that favor incisive fluvial sediment transport styles coupled with incisive base level conditions, pediment development will be hampered by a roughening of sediment mantled surfaces, thereby creating spatial variability in topography, regolith thickness, and bedrock weathering rates. In addition, when base level incision rates, governed by tectonics or climatic conditions, exceed the integrated sediment flux along a hillslope derived from upslope weathering, hillslopes and mountain masses will remain bare and will lack footslope pediments.

We have also hypothesized that hydrologically-closed basins maintaining residual mountain masses are less likely to build footslope pediments than those basins that are hydrologically-open (Strudley et al., 2006a). Climatic conditions that engender deep (**O** (10^1 m)) or spatially variable regolith profiles via accelerated groundwater or dissolution-type bedrock-weathering processes will also limit the development of pediment landforms.

This paper begins with a brief recapitulation of our numerical model, with particular emphasis on the implementation and description of various initial conditions, the incorporation of spatial variability in lithology, various base level histories, variation in rainfall rate, and modifications to soil properties, sediment transport styles, and subsurface bedrock weathering. We follow with a description of our model sensitivity analysis and simulation results, illustrating under what conditions our model permits (or restricts) pediment development. To test predictions made by the sensitivity analysis, we examine field sites across the southwestern United States for the presence or absence of pediment landforms. We provide more detailed descriptions of sites we have visited, and give brief descriptions for unvisited sites for which either satellite imagery or USGS 7.5′ quadrangle geologic maps indicate or suggest the presence of pediment surfaces. Our discussion then illustrates the limitations in the predictive capabilities of our model and in our 'geospatial query' for pediment landforms. Based on the implications of this sensitivity analysis, we also provide a process-based definition for the term 'pediment' to quell a long-standing confusion surrounding the selection of an appropriate definition. Our primary objective with this work is to outline conditions in which our model predicts the presence or absence of pediment landforms, and to provide a brief description of further tests using refined models, geospatial data, and fieldwork to test model predictions. We do not intend to provide an exhaustive and definitive list of conditions in which pediments prevail, but our work suggests general constraints, illustrated through numerical modeling, imposed on the development of pediment landforms.

2. Numerical model

Our model consists of a grid of cells (grid and cell size vary and are specified in figure captions) with cell-centered sediment (regolith) and bedrock elevation and regolith-thickness attributes that evolve according to regolith formation, diffusive hillslope sediment transport, and fluvial sediment transport (Strudley et al., 2006a). We intend to model the development of pediments along the footslope of evolving mountain range fronts.

2.1. Bedrock weathering

Bedrock surfaces are modified through time by weathering processes controlled by the overlying thickness of regolith. We model the production of regolith (Fig. 1A) using a bedrock weathering rule motivated by field observations that suggest that a limited regolith cover enhances the weathering rate relative to bare bedrock (Gilbert, 1877; Carson and Kirkby, 1972; Cox, 1980; Furbish and Fagherazzi, 2001; Anderson, 2002; Dietrich et al., 2003), highlighting the importance of mineral hydration and chemical weathering afforded by water retention in thin layers of regolith cover (Wahrhaftig, 1965; Oberlander, 1972):

$$W(h) = \gamma\varpi_o(e^{-h/d_1} - k_1 e^{-h/d_2}), \tag{1}$$

where, $W(h)$ is the bedrock weathering rate (m Ma^{-1}) as a function of regolith thickness h (m), ϖ_o is a constant (=70 m Ma^{-1}), d_1 and d_2 are decay scaling factors (m) that control the shape and position of the declining limb of the regolith production curve, k_1 is a dimensionless coefficient (=0.8) that determines the magnitude of the bare-bedrock weathering rate relative to ϖ_o, and γ is a factor used to illustrate alterations to ϖ_o when the model incorporates spatial variability in lithology, as described below. Weathering rate parameters are chosen so that the magnitude and functional form of the weathering curve approximate values obtained by measuring the concentrations of cosmogenic radionuclides as a function of depth below the surface from bedrock samples in arid/semiarid environments (Granger et al., 1996, 2001; Nichols et al., 2005) and in other environments possessing granitic and sedimentary tors that often punctuate and signal the presence of pediments (Heimsath et al., 1999, 2000; Wilkinson et al., 2005). Using a "non-humped" regolith production curve (Heimsath et al., 1997) prevents tors from developing in our model but does not alter the process rates or implications of our sensitivity analysis as long as maximum weathering rates for both types of curves are equal.

We introduce perturbations to this simple depiction of bedrock weathering by either incrementally increasing d_1 in Eq. (1) or by introducing spatially variability in ϖ_o through the term γ in Eq. (1). The former perturbation raises the tail of the regolith production curve while maintaining the same bare-bedrock weathering rate (Fig. 1B), parameterizing the case in which moist environments potentially accelerate deep regolith production through higher fluxes and longer residence times of subsurface moisture and groundwater. The latter perturbation (spatial variability in ϖ_o through γ) simulates conditions in which mountain masses and hillslopes in our model consist of more than one rock type. Specifically, we build upon prior modeling work that simulated irregular spatial perturbations to both lithology and topography (Strudley et al., 2006a) by including layered sedimentary rock in various orientations. We model initial conditions consisting of alternating layers of sandstone and shale/siltstone, each either 3 m or 15 m thick, and resting 1) horizontally, 2) vertically and parallel to the range front, 3) vertically and perpendicular to the range front, and 4) in a dip-slope position. Layer thicknesses were chosen arbitrarily to represent cases in which thin layers (3 m) and thick layers (15 m) model two "end member" levels of spatial variation and repetition in rock type across a model domain of fixed dimension. Sandstone layers are modeled with $\gamma = 1$, and shale layers are modeled with $\gamma = 3$, the latter representing more easily erodible layers of fine-grained, fissile shales and siltstones. The hydrologic properties of the regolith generated from the specific layers differ as well, with parameter values described below.

2.2. Hydrology

We calculate runoff across our model domain based on rainfall intensity, rainfall duration, and infiltration. In our previous modeling endeavor describing pedimentation (Strudley et al., 2006a), we selected effective storm intensities, i (m h^{-1}), and durations, t (h storm^{-1}), using hourly precipitation records for stations in the Mojave Desert, California (Baker, Iron Mountain, Mojave, Needles, and Victorville) and Bakersfield, California (NOAA, 1999). The number of storms per year, n, was also constrained by these precipitation records. Here, we simulate different climatic environments (arid and temperate/humid) characterized by "end-member" rainfall regimes derived from generalized isohyetal maps of the coterminous United States (Dunne and Leopold, 1978): 1) high intensity storms in arid environments (10-year recurrence interval; $i=0.076$, $t=0.5$); 2) high intensity storms in humid environments (10-year recurrence interval; $i=0.102$, $t=0.5$); and 3) low intensity storms in humid environments (2-year recurrence interval; $i=0.004$, $t=24$). Low intensity storms in arid environments (2-year recurrence interval; 24-hour duration) with an "end-member" rainfall intensity i of ~ 0.002 fail to generate runoff for regolith profiles thicker than ~ 0.1 m (see infiltration rules below), creating regolith-mantled parabolic profiles controlled by hillslope diffusion and extending to the hillslope crest, thus preventing footslope pediment development and warranting their exclusion from our sensitivity analysis. Indeed, our experiences in the field, including witness to mild storms in the Mojave Desert, CA, suggest that arid piedmont environments characterized by unconsolidated gravels and sands require excessive rainfall intensities to generate surface runoff. For each type of environment and rainfall regime (humid-high intensity, arid-high intensity, or humid-low intensity), we vary the total amount of annual rainfall by incrementing the total number of storms per year, n. In humid environments, we vary n from 4–100 using high intensity storms and from 2–50 using low intensity storms, spanning rainfall rates from as little as 8 in. per year up to 200 in. per year. In arid environments, n ranges between 3 and 20, equivalent to a range in average annual precipitation of ca. 100–750 mm. This range in average annual rainfall envelops conditions across the coterminous United States (Daly et al., 1994).

Infiltration plays a role in damping a downslope increase in runoff magnitude with drainage area, thus its calculation is pertinent in determining runoff fluxes along piedmonts. We calculate infiltration depths explicitly at the time scale of individual storms by using a rearrangement of the Green–Ampt equation (Bedient and Huber, 1992), which predicts the depth of infiltration reached prior to surface saturation:

$$F = -\psi_{\mathrm{f}}(\theta_{\mathrm{s}}-\theta_{\mathrm{u}})/(1-i/K_{\mathrm{s}}), \tag{2}$$

where F is the infiltration depth that occurs implicitly over the course of a storm (m), ψ_{f} is the wetting front soil suction head (m), θ_{s} is the saturated sediment porosity, θ_{u} is the unsaturated sediment porosity, and K_{s} is the saturated hydraulic conductivity (m h^{-1}) of the sediment. Infiltrated water is assumed to ultimately evaporate (in desert environments), or to contribute to deep groundwater reservoirs (in temperate/humid environments). Parameter values vary depending on the moisture regime (humid or arid), and on the rock type involved in weathering processes. Specifically, we use tabulated parameter values (Bedient and Huber, 1992) based on 1) sand-sized particles for arid environments and the regolith derived from sandstones and crystalline igneous rocks: $\psi_{\mathrm{f}}=-0.05$, $\theta_{\mathrm{s}}=0.4$, $\theta_{\mathrm{u}}=0$, and $K_{\mathrm{s}}=0.03$, and 2) silt- and clay-sized particles for humid environments and the regolith derived from shales/siltstones: $\psi_{\mathrm{f}}=-0.3$, $\theta_{\mathrm{s}}=0.4$, $\theta_{\mathrm{u}}=0$, and $K_{\mathrm{s}}=0.0005$. For humid environments, the soil hydraulic parameter values reflect the effect of higher soil moisture content on the style and intensity of bedrock and regolith weathering, in which more complete disintegration, alteration, and dissolution of crystalline materials yield silts and clay minerals (Riebe et al., 2004) that reduce infiltration rates. In our infiltration model, when $i \le K_{\mathrm{s}}$, rainfall infiltrates until the regolith column's porosity is exceeded or until the rainfall is completely absorbed. When $i > K_{\mathrm{s}}$, we compare the calculated infiltration depth, F, and the available pore space in the regolith column ($h\theta_{\mathrm{s}}$), which is limited by local regolith thickness. If the pore space presents no limit to the calculated F, rainfall infiltrates. Otherwise, a volume infiltrates per unit area that is equal to the available pore space, with the remaining water, if any, contributing to runoff. Runoff out of each cell for both scenarios ($i \le K_{\mathrm{s}}$ and $i > K_{\mathrm{s}}$) is then

$$q_{\mathrm{w}} = it\Delta x - \min(F\Delta x, h\theta_{\mathrm{s}}\Delta x) = q_n, \tag{3}$$

where q_{w} is the volumetric runoff per unit width per storm (m^2 storm^{-1}), q_n is the volumetric runoff per unit width per storm arriving in the cell from upstream neighbors (m^2 storm^{-1}), and Δx is the cell size (m). This calculation of runoff allows us to model Hortonian and saturation overland flow in regolith mantled domains, while on bare bedrock there is no infiltration. The model discharges represent summations over the total discharges in channels that are implicit within each cell.

2.3. Sediment transport

Cells are sorted by elevation and are subjected, in order of descending elevation, to sediment transport processes. Across each nearest-neighbor cell boundary, diffusive transport moves sediment downslope (Fernandes and Dietrich, 1997) according to:

$$q_{s,d} = k_2 S, \tag{4}$$

where $q_{s,d}$ is the volumetric diffusive sediment flux per unit width ($m^2\ y^{-1}$), S is the slope between the centers of adjacent cells, and k_2 is the diffusivity coefficient ($1\times10^{-3}\ m^2\ y^{-1}$) (Hanks et al., 1984).

Fluvial sediment transport distributes sediment fluxes proportional to slope and runoff (Carson and Kirkby, 1972; Vanoni, 1975; Howard, 1994):

$$q_{s,f} = k_3 q_w^{\alpha} S^{\beta}, \tag{5}$$

where $q_{s,f}$ is the volumetric fluvial sediment flux per unit width per storm ($m^2\ storm^{-1}$), k_3 is a transport efficiency parameter, and α and β are constants ($k_3 = 1\times10^{-3}\ m^{2-2\alpha}\ storm^{-(\alpha-1)}$ or $1\times10^{-5}\ m^{2-2\alpha}\ storm^{-(\alpha-1)}$, $1.1 \le \alpha \le 2.0$, and $\beta = 1$ in runs reported here). We vary the relative strength of fluvial to diffusive sediment transport by varying the style and amount of precipitation through i, t, n, by varying α, and by varying infiltration parameters. The transport efficiency parameter varies according to the modeled environment: in arid environments, k_3 is 1×10^{-3}; whereas, in humid environments, we lower k_3 to 1×10^{-5} to suppress numerical instabilities that accompany larger k_3 and α values while using cell sizes ranging from 3–25 m and a time step of 2 y. Hydraulic routing is performed according to the $D\infty$ algorithm of Tarboton (1997).

We multiply the sediment fluxes for each storm type by the number of storms of that type per year (n) and by the time step (2 years). We treat sediment erosion and accretion as if they were distributed evenly throughout a cell, reflecting the long timescales of the model and the tendency for channels on pediments to migrate laterally (Nichols et al., 2002). Sediment surface elevations are adjusted according to the difference of diffusive and advective fluxes in and out of each cell, while bedrock elevations are decreased according to the weathering rule $W(h)$.

2.4. Initial and boundary conditions

Initial conditions in most runs consist of a bedrock plane inclined at ~22°, seeded with white-noise elevation perturbations of (**O**) m, and mantled by 5–10 m of regolith cover (Howard, 1994; Anderson, 2002). Some simulations model larger landscapes 400 m wide by 2000 m long, while others are 48 m wide by 240 m long and use an initial slope of ~5° to test the piedmont's sensitivity to variations in sediment transport style and soil hydrologic response, i.e., modifications to soil hydraulic properties and α in Eq. (5). The captions of some figures note these digressions in domain size and initial geometry. We selected an initial regolith thickness value sufficiently high to avoid artificially limiting infiltration volumes by an insufficiently thick regolith cover. In this way, the effects of high rainfall and runoff rates in more humid environments can more realistically place their geomorphic signature upon the landscape, rather than prematurely strip a thinly mantled hillslope of its regolith cover. The lower boundary condition is "open", meaning that the sediment elevation is either fixed or decreasing, the latter representing incision. We couple various magnitudes of base level incision rate to our simulations modeling various magnitudes of average annual precipitation, with base level incision rates ranging between 0 and $10^{-2}\ m\ y^{-1}$. Simulations incorporating hydrologically-closed boundary conditions are presented elsewhere (Strudley et al., 2006a), and restrict pediment development until the mountain mass has completely weathered away. Lateral boundary conditions are periodic and permit fluxes of runoff and sediment, thus eliminating the propagation of boundary condition effects into the model domain, which could potentially alter the evolving landscape form.

3. Simulation results

3.1. Lithologic variability: layered sedimentary rock

Our simulation results illustrating the effect of lithologic variability in the form of alternating layers of sandstones and shales/siltstones are shown in Fig. 2A–F. Fig. 2A,B show how horizontally layered sedimentary rocks do not prevent the development of a smooth pediment surface characterized by a spatially uniform equilibrium regolith mantle. The longitudinal profile views at the top of Fig. 2A,B exhibit stepped bare-bedrock profiles for the evolving mountain mass,

Fig. 2. Simulation results illustrating the effect of lithologic variability in the form of alternating layers of sandstones and shales/siltstones in various orientations. Longitudinal profile views included above oblique views for simulations depicted in panels A through E. Horizontal scale bar and regolith thickness color bar in panel F applies to all panels. Simulation durations (t) shown below landform. Horizontally-layered sedimentary rocks with (A) 3-meter layer thickness and (B) 15-meter layer thickness. Dip-slope layered sedimentary rocks with (C) 3-meter layer thickness and (D) 15-meter layer thickness. Vertically-layered sedimentary rock oriented (E) parallel and (F) perpendicular to the range front; layer thickness is 3 m.

while variations in weathering rates beneath the pediment surface do not drastically affect the development of a spatially uniform regolith mantle. Regolith profiles vary by only (**O**) m (Fig. 2A,B), with slow-weathering sandstones forming thinner mantles than those overlying the faster-weathering shales/siltstones

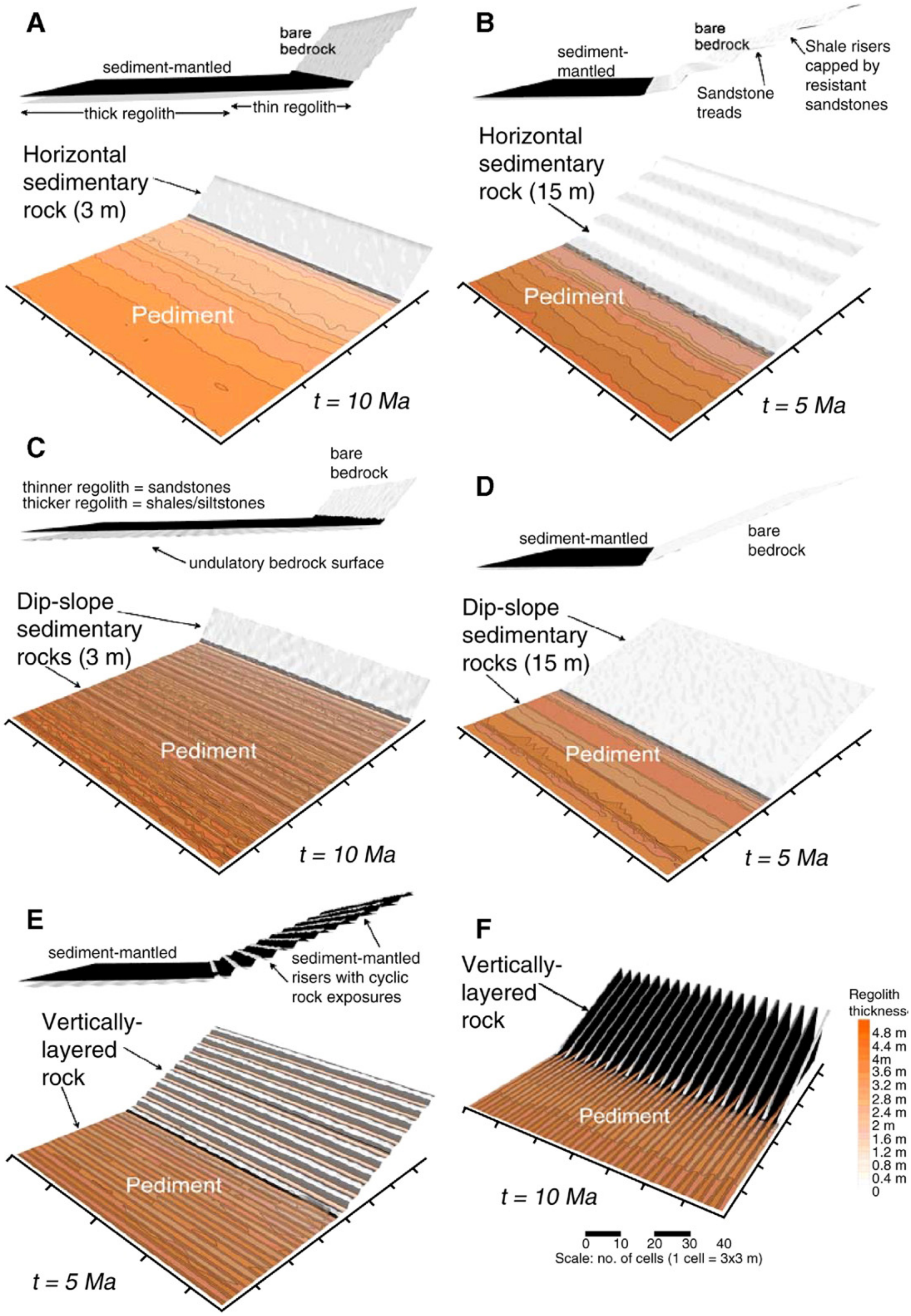

(Fig. 2A profile). The extent to which alternating depths of equilibrium regolith profiles on the pediment develop depends on the frequency of intersection of the weathering front (controlled by the pediment's slope) and the horizontal rock layers (controlled by the layer thickness). Because pediment slopes remain minute even for high rainfall rates (see below), variations in regolith thickness caused by alternating layers of horizontal rocks will be infrequent for very thick rock layers (many meters). Although very thin rock layers (less than 1 m) potentially create high frequency variability in regolith thickness across a pediment, repetition of parallel rock layers creates low spatial variability, especially as pediment size increases.

Fig. 2C,D illustrate the effect of alternating rock layers positioned in a dip-slope orientation. Regolith thickness again varies cyclically away from the mountain front (as in Fig. 2A,B), with the frequency controlled by the rock-layer thickness. Here the perception of a spatially uniform regolith mantle may be disrupted if the disparity between the rock layers' weathering rates is great. Our simulation results show, however, that varying the weathering rates up to 3-fold for sandstones versus shales/siltstones creates a standard deviation in regolith thickness across the developing pediment of only ±0.47 to ±0.63 m for layer thicknesses ranging from 3 to 15 m, respectively, over the course of millions of years. The results of incorporating vertical rock layers oriented parallel and perpendicular to the range front (Fig. 2E,F) illustrate a similar pediment morphology to those shown in Fig. 2C,D, and exhibit the same effects on pediment-wide equilibrium regolith thickness as a function of rock-layer thickness. The landscape developed in Fig. 2F, however, has a drastically different evolving mountain-front morphology defined by the orientation of the vertical rock layers. Here, the piedmont junction, or slope discontinuity that separates the evolving mountain front from the developing pediment below, oscillates in basinward position along the range front, creating cyclic embay-

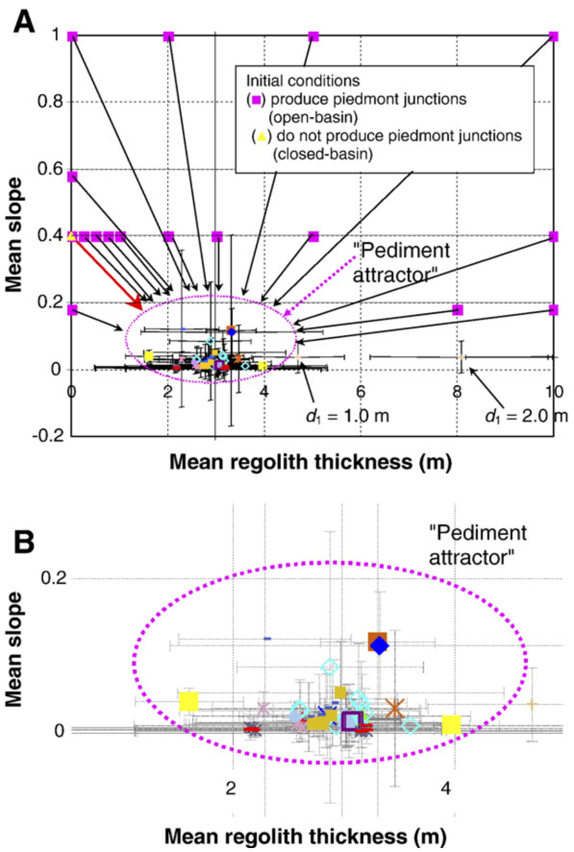

Fig. 3. Modified "pediment attractor" diagram (A) and closeup (B) from Strudley et al. (2006a) illustrating the mean regolith thickness and mean slope of pediments developed in numerical simulations. Points are plotted within a "state space" defined by the regolith thickness and slope. Initial conditions are plotted as either those models that produce piedmont junctions (open-basin boundary conditions, magenta squares) or those that do not (closed-basin boundary conditions, yellow triangles). Data points for simulations modeling layered sedimentary rock, alterations to d_1, and alterations to rainfall rates, sediment transport style, and base level incision rates included here. Note that increasing d_1 in Eq. (1) in the text results in a mean regolith thickness outside of the "pediment attractor." The pediment data are obtained from an algorithm that selects cells within each simulation that exhibit regolith thicknesses between 0.0001 and 6.0 m; 4-point nearest-neighbor gradients are calculated and averaged for these cells, and averages are calculated for the regolith thicknesses. Horizontal and vertical error bars represent ±1 standard deviation in pediment's regolith thickness and slope, respectively. The thick, red arrow represents multiple simulations that begin with slopes of 0.4 (22°) and zero sediment thickness and the black arrows represent all other simulations. Other symbols represent evolved pediments as follows: Evolved pediments: (■) simple decaying exponential $W(h)$; (▲) $k_3=0.0007$ or 0.003; (◊) initial slope=10–45°, sediment thickness=0–10 m; (□) randomly-placed 0–3 m elevation perturbations; (X) doubly-sinusoidal elevation perturbations; (▲) elliptic paraboloid elevation perturbations; (*) spatially-random perturbations of lithology; (■) weathering rates vary spatially by 3-fold (14 m Ma$^{-1} \le \omega_o - k_1\omega_o \le 42$ m Ma^{-1}) in a "checkerboard" pattern; (+) elliptic paraboloids defining elevation perturbations; elliptic paraboloids defining variations in lithology; (♦) highly non-linear sediment transport (α=2.0), spatially-limited storm footprints; (•) weakly non-linear sediment transport; 4.5, 15, 30 in. annual rainfall; (■) strongly non-linear sediment transport; high and low intensity storms; 8, 20, 40, 80, and 200 in. annual rainfall; (●) annual rainfall (0–20 in.) and base level incision (0–0.004 m y^{-1}) forced by orbital cycles (precession, obliquity, eccentricity, insolation); (+) varying d_1 (regolith production function) from 1.0–6.0 m; (-) sedimentary strata (vertical, horizontal; 3 m- or 15 m-thick alternating layers of sandstone and shale); (X) strongly non-linear sediment transport; high intensity storms; 8, 20, 40, 60, 80, and 100 in. annual rainfall, with base level incision (**O** (10^{-4} m y^{-1})); (-) strongly non-linear sediment transport; low intensity storms; 8, 20, 40, 60, 80, and 100 in. annual rainfall, with base level incision (**O** (10^{-4} m y^{-1})).

ments and promontories. Note that although promontories are formed from the more resistant layers, the pediment surface indiscriminately planes all rock layers, as found in nature (e.g., Rich, 1935).

3.2. Climatic variability: effects of high moisture availability on deep regolith production

As expected, increasing d_1, which would accelerate bedrock-weathering processes at depth, leads to the development of deeper regolith mantles on the piedmont and loss of diagnostic pediment morphology. This represents cases, for example, in which a portion of underlying bedrock may be composed of biochemical rocks such as limestone (Eppes et al., 2002; Pearce et al., 2004) and be subject to dissolution; or cases in which granitic or other types of rock may be subject to higher potential groundwater residence times in more humid environments (Beauvais et al., 2003). As d_1 is increased from 0.5 to 6.0 m, piedmont regolith thickness escalates from a piedmont-averaged 3.02 ± 0.49 to 26.00 ± 6.37 m (Figs. 3A and 4). Here, an erosional footslope landform, with lowering, coupled alluvial and bedrock surfaces, possesses an exceptionally thick regolith profile, lending its morphology more reminiscent of an alluvium

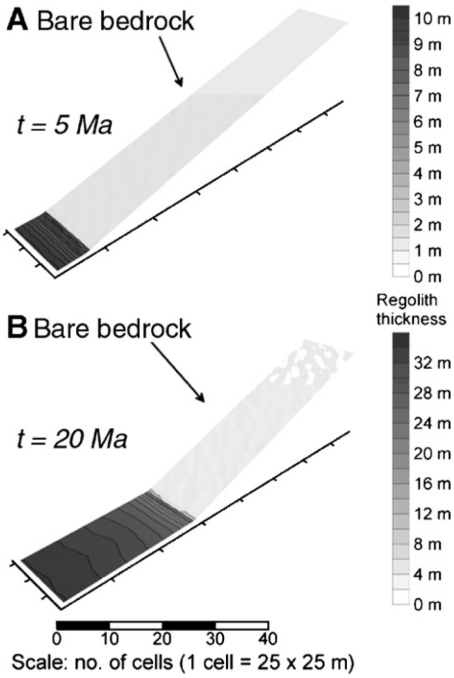

Fig. 4. Simulation results illustrating the effect of increasing d_1 in Eq. (1). Regolith thickness becomes exceedingly great on the piedmont with increasing d_1. (A) $d_1 = 2.0$ m. (B) $d_1 = 6.0$ m. Note that although the model durations increase from panels A to B, these are two separate model runs.

fan deposit. Thus, although the dynamics of such a landform is the same as that of a pediment, its morphology precludes its identification as a pediment landform.

3.3. Climatic variability: pediment development in arid and humid environments

Footslope pediment development in arid environments with hydrologically-open boundary conditions proceeds unencumbered as long as rainfall rates are sufficient to maintain bare-bedrock uplands. In humid environments with hydrologically-open boundary conditions, pediment development also remains relatively unaffected by the effects of more cohesive sediments that foster strongly non-linear fluvial sediment transport style (Fig. 5A–F). Fig. 5A,D illustrate that at low simulated rainfall rates of 20 cm y^{-1}, the entire landscape remains mantled and a bare-bedrock upland does not develop. Additionally, these two simulations illustrate slight channelization and tor development (Strudley et al., 2006b). At higher rainfall rates, channelization appears more suppressed or absent, the result of a fixed elevation boundary condition combined with widespread Hortonian overland flow that overwhelms localized channelization. Although Fig. 5C,F illustrate the development of smooth surfaces despite high rainfall rates and strongly non-linear fluvial sediment transport style, we do not suggest that environments characterized by such hydrology often support smooth pediment surfaces. Our results merely imply that even for high rainfall rates in hydrologically-open basins, pedogenic, ecologic, and/or bedrock incision processes not captured by our model, along with base level conditions (see below), may play a more dominant role in suppressing pediment development in humid environments than high rainfall rates alone.

Fig. 5G–P illustrate simulations in which semi-arid to humid environments experience base level incision of (**O**) 10^{-4} m y^{-1}. At low to moderate rainfall rates (~20–50 cm y^{-1}; Fig. 5G,H,M,N), base level incision combined with a strongly non-linear fluvial sediment transport algorithm produces visible channel systems that roughen sediment mantled surfaces. With higher rainfall rates (Fig. 5I–L,O–P) channelization instigates regolith thickness instability (Strudley et al., 2006b), which forms tors and inselbergs. Because the lateral boundary conditions in the model are periodic, streams often course laterally across the model domain, forming lineaments of regolith thickness instability and tor growth laterally across the simulated landscapes. In some cases (Fig. 5H–J,L,N–P), these bedrock "ribbons" provide temporary local base levels for regolith mantled domains upslope, with lowering rates controlled by the number and width of through-flowing streams and the bare-bedrock weathering rate. These bedrock ribbons create a stepped topography with disconnected pedimented surfaces roughened by fluvial incision and punctuated by tors, and may represent a model analogue to the stepped topography of the southern Sierra Nevada described in detail by Wahrhaftig (1965).

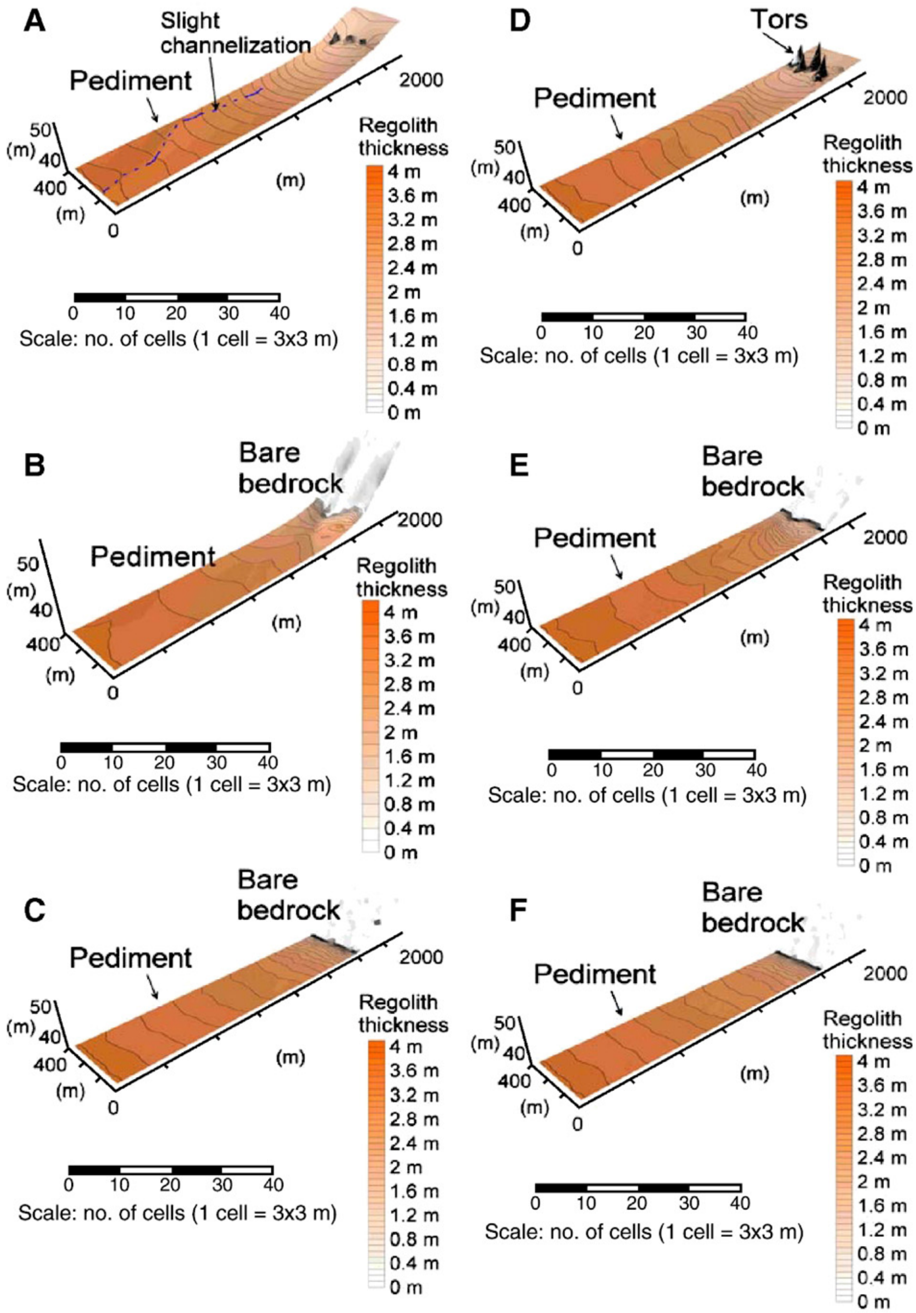

Fig. 5. Simulation results after 5 Ma using various rainfall magnitudes for both low intensity (panels A–C; G–L) and high intensity (panels D–F; M–P) storms in humid environments (strongly non-linear fluvial sediment transport rule). Panels A–F exhibit hydrologically-open base level; panels G–P exhibit base level incision (**O**) 10^{-4} m y^{-1} and an initial slope of ~5°. (A) 20 cm y^{-1}; (B) 50 cm y^{-1}; (C) 508 cm y^{-1}; (D) 20 cm y^{-1}; (E) 50 cm y^{-1}; (F) 508 cm y^{-1}; (G) 20 cm y^{-1}; (H) 50 cm y^{-1}; (I) 102 cm y^{-1}; (J) 152 cm y^{-1}; (K) 254 cm y^{-1}; (L) 508 cm y^{-1}; (M) 20 cm y^{-1}; (N) 50 cm y^{-1}; (O) 102 cm y^{-1}; (P) 152 cm y^{-1}.

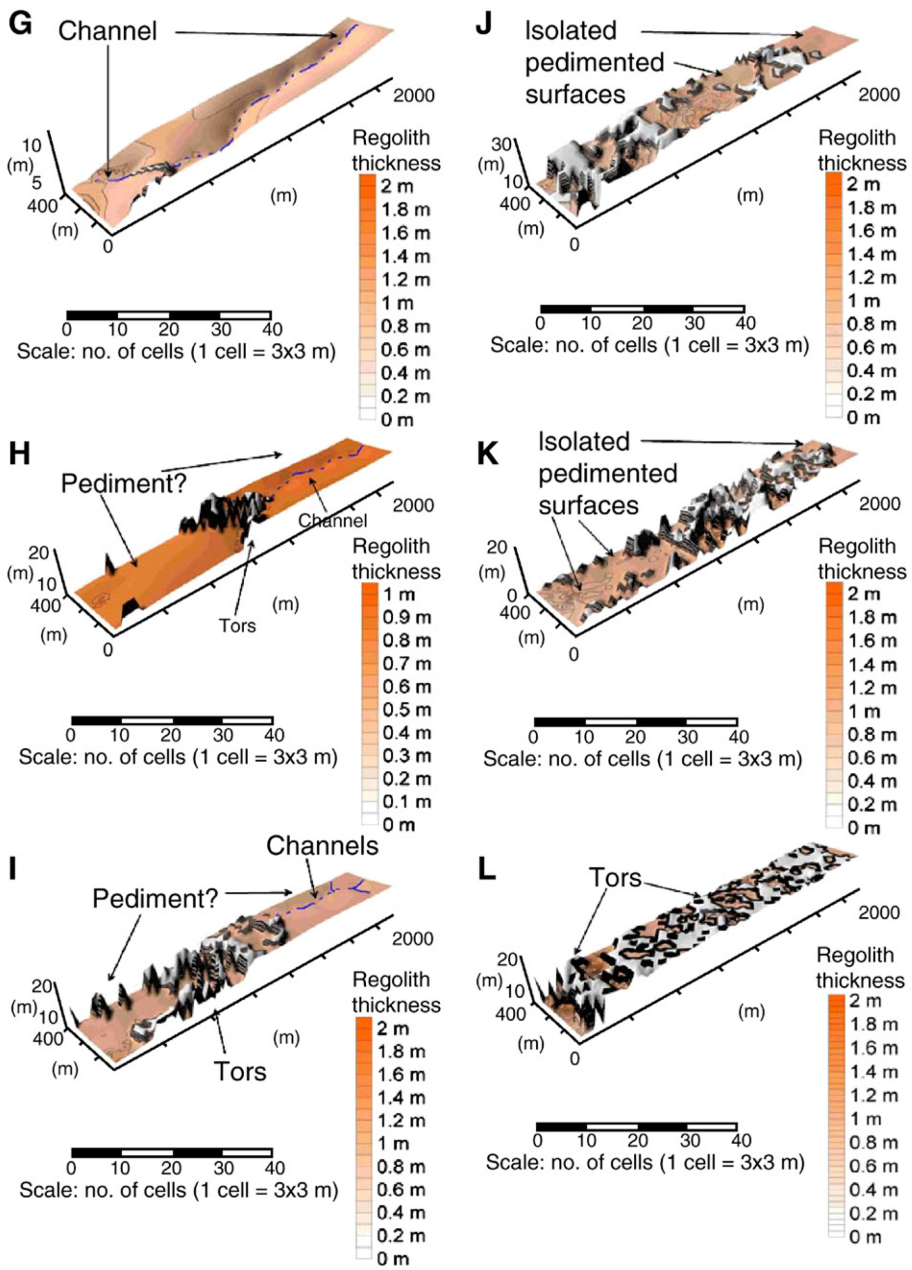

Fig. 5 (*continued*).

The end result of employing a highly non-linear fluvial sediment transport rule coupled to finite base level incision is a roughened, disjointed surface that locally exhibits pediment-like equilibrium regolith profiles but diverges as a whole from the characteristic pediment morphology. As base level incision rates approach 10^{-3} m y^{-1}, the integrated sediment flux reaching the basin boundary is transmitted away, leaving a bare-bedrock slope lacking footslope pediment development.

4. Testing model predictions using field data, geologic maps, and satellite imagery

Model simulations predict that moist climatic conditions that engender deep (**O** (10^1 m)) or spatially variable regolith profiles via accelerated bedrock-weathering processes at depth limit the development of pediment landforms. Likewise, models simulating a more humid environment supporting incisive fluvial sediment

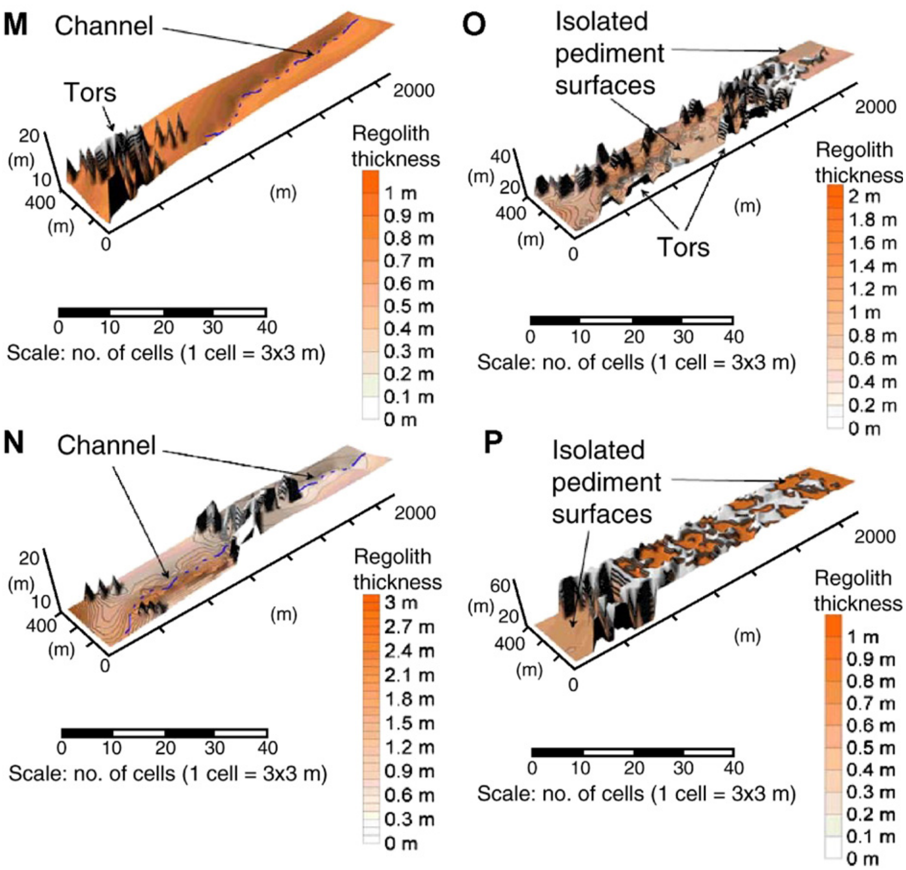

Fig. 5 (*continued*).

transport style through moisture-controlled soil and vegetation characteristics, coupled with base level incision, predict limited pedimentation. Additionally, when base level incision rates, governed by tectonics or climatic conditions, exceed the integrated sediment flux along a hillslope derived from upslope weathering, hillslopes and mountain masses will remain bare and will lack footslope pediments. Our model also indicates that hydrologically-closed basins maintaining residual mountain masses are less likely to build footslope pediments than those basins that are hydrologically-open (Strudley et al., 2006a), while pediment domes or passes represent the ultimate developmental state in both hydrologically-open and -closed basins (Strudley et al., 2006a).

A comprehensive test of the predictions made by our model of pediment development would require geospatial data describing the full range of diagnostic characteristics of pediments (slope and regolith thickness) as well as prognostic data, including base level history and climatic attributes (rainfall rates; vegetation type and density; soil hydrologic properties; and style and intensity of bedrock weathering). Regolith thickness and base level history data are unavailable at most sites, however, and the coarseness in resolution of regional climatic, vegetation, slope, and soil geospatial datasets renders a comprehensive geographic query futile. Instead, we test our model predictions at various field sites underlain by mostly granitic and gneissic rocks in the arid and semiarid southwestern United States, where climatic parameters (vegetation, soils, rainfall, and weathering) are known and almost constant, and base level conditions can be ascertained in the field or by using topographic maps and satellite imagery. In addition, we also utilized four USGS 7.5′ quadrangle geologic maps in the Mojave Desert of southern California and the Colorado Desert along the Nevada–Arizona state line in which highly detailed geomorphic mapping indicates the presence of a number of pediment surfaces.

4.1. Field sites: climate and geology

Our field sites in the USA (Fig. 6) include Joshua Tree National Park, California (Fig. 7A), the Sacaton

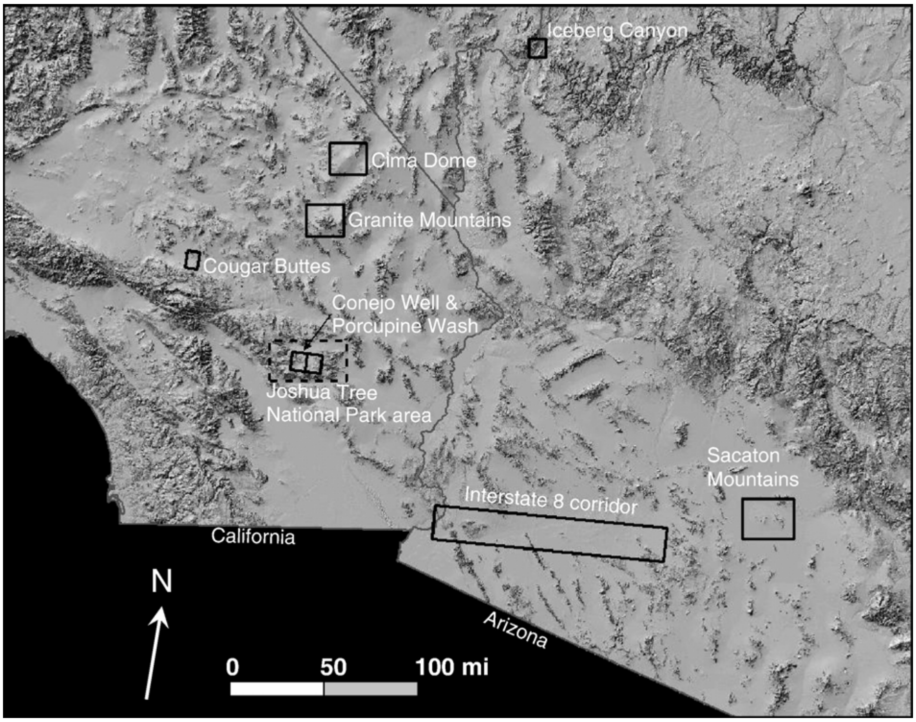

Fig. 6. Field sites and geologic map locations used in model prediction tests identified on USGS NED shaded relief map of the southwestern United States. Boxes for geologic map sites exactly identify the quadrangle location and position. Other sites approximately identified.

Mountains in Arizona (Fig. 7B), the Granite Mountains (~34°50′00″ N; ~115°40′00″ W) (Fig. 7C) and Cima Dome (Fig. 7D) in the Mojave Desert, California, as well as numerous other pediment landforms intersected by Interstate Highway 8 crossing southwestern Arizona from the Pinal–Maricopa County line to Yuma, Arizona. We also analyze data from the Conejo Well (Cossette, 2001a; Powell, 2001a) and Porcupine Wash (Cossette, 2001b; Powell, 2001b) geologic quadrangle maps in the Joshua Tree Wilderness, California; the Cougar Buttes quadrangle geologic map in Lucerne Valley, California (Cossette, 2000; Powell and Matti, 2000); and the Iceberg Canyon quadrangle geologic map in Clark County, Nevada and Mohave County, Arizona (Brady et al., 2002).

All field sites and locations described by geologic quadrangle maps receive little annual rainfall, and in general exhibit loose, unconsolidated grus supporting sparse mesic and xeric vegetation (creosote, ocotillo, saguaro, jumping cholla, etc.). The San Bernardino and Little San Bernardino Mountains shelter the Mojave Desert from most Pacific winter cyclones, and annual rainfall rarely exceeds 100 mm (Oberlander, 1972; NOAA, 1999). The Sonora Desert in southwestern Arizona receives little annual rainfall as well, but is subject to intense rainfall during the summer monsoon in July and August. Carbonate development in the soil is minimal, and most surface clasts lack desert varnish. Ephemeral washes are responsible for most downslope sediment transport on piedmont surfaces (Bull, 1977), and small mammal burrows disrupt regolith profiles to depths less than or equal to ephemeral channel scour (Nichols et al., 2002). Downslope transport of sediment particles by rainsplash plays a small but significant role in identical and similar arid/semiarid environments where vegetative stabilization and protection are lacking (Dunne and Aubry, 1986; Jyotsna and Haff, 1997).

Monzogranite, granodiorite, and adamellite of Mesozoic age dominate the granitoid lithology of the Mojave Desert of southern California (Miller et al., 1991), while Pre-Cambrian granite, quartz monzonite, granodiorite, quartz diorite, and gneiss underlie the Sacaton Mountains in Arizona (Bryan, 1922; Hirschberg and Pitts, 2000). The surveyed I-8 corridor in southwestern Arizona crosses a mixture of Mesozoic granite and quartz diorite, gneisses, Tertiary sedimentary rocks, isolated Tertiary and Quaternary volcanic flows, and metasedimentary rocks (Hirschberg and Pitts, 2000). The Iceberg Canyon quadrangle, straddling the Nevada–Arizona state line near Lake Mead, consists predominantly of Quaternary and Tertiary basalts and sedimentary rocks, and Paleozoic sedimentary rocks of various types (Hirschberg and Pitts, 2000; Stewart et al., 2003).

4.2. Field sites: description of pediments and local drainage

Cima Dome forms an expansive pediment dome in the eastern Mojave Desert with approximately linear side slopes (Sharp, 1957; Boring, 1999) exhibiting a network of ephemeral channels with depths of centimeters to decimeters and widths on the order of decimeters to a meter (Sharp, 1957; Nichols et al., 2002). Tors are prevalent near the apex of the dome, and distally disappear towards the surrounding basins and washes. The pediment surface surrounding and including the dome apex exhibits spatially uniform regolith mantles of coarse grus (**O** (m)), while distal portions of the dome on the southeast side can exhibit alluvial thicknesses in excess of 150 m (Sharp, 1957). The Ivanpah Valley to the northeast, the Shadow Valley to the northwest, and the Kelso–Cedar Wash drainage system to the south and southwest form a mixture of hydrologically-open and -closed boundary conditions surrounding Cima Dome, although numerous desert washes traversing the dome and Pleistocene lava beds to the west complicate local boundary conditions.

A large pediment on the southeastern flank of the Granite Mountains exhibits similar drainage network morphology to that of Cima Dome, but in general supports a much higher spatial density of tors, with tor fields often extending the length of the piedmont to desert washes below. Regolith thickness is on the order of a meter along the SSE pediment surface, whereas bare and incised pediments inhabit areas near the Willow Spring Basin south of the Granite Mountains. Desert washes follow Kelbaker Road southwest around the south-southeastern most pediments, eventually feeding incised channels and washes associated with Interstate 40 drainage diversions along the southern periphery of the Granite Mountains piedmont.

Joshua Tree National Park exhibits numerous tor-studded pediment surfaces and domes in the Lost Horse and Queen Valleys and in Pinto Basin, although there are likely numerous other pediments not visited by us or currently mapped within the park. A variety of granitic rock types preserve both thickly mantled pediments (**O** (m)), exhibiting poorly developed piedmont junctions, and thinly mantled or bare pediments possessing numerous tors and inselbergs (i.e., in Lost Horse Valley

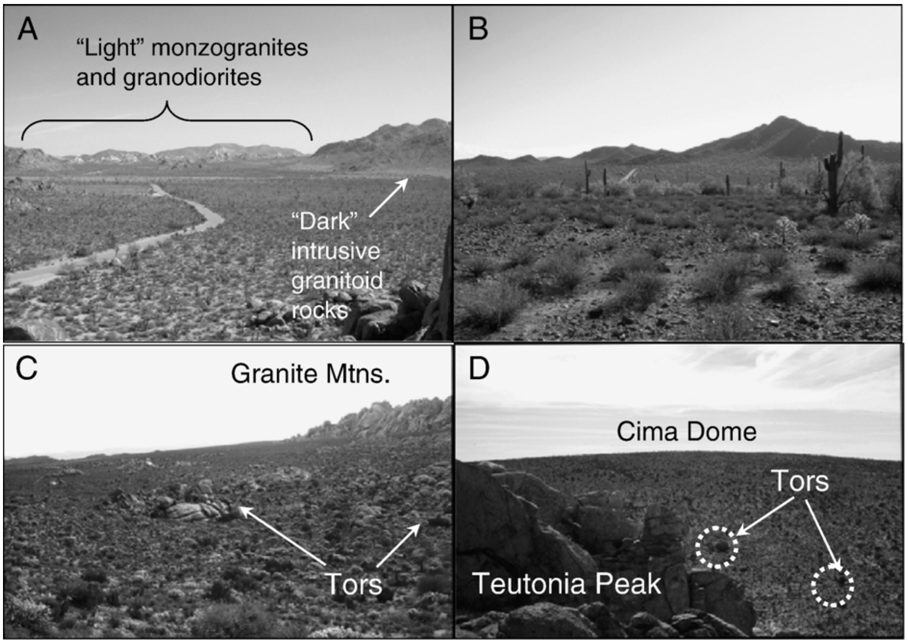

Fig. 7. Images of field sites. (A) View looking southeast along Quail Springs Road in Joshua Tree National Park, CA. Note the light-colored monzogranites and granodiorites on the left, and the dark-colored granitoid rocks on the right. The former forms abundant tors and inselbergs within pediment surfaces bounded by sharp piedmont junctions, while the latter does not tend to produce tors or inselbergs within pediments bounded by less distinct piedmont junctions. (B) Sacaton Mountains (background) and pediment (foreground), just southwest of Phoenix, AZ. Again, note lack of tors and less distinct piedmont junctions. (C) Granite Mountains pediment, looking roughly southeast. Local drainage is off left side of photograph. (D) View of Cima Dome, Mojave Desert, CA, from the top of Teutonia Peak, a resistant residual on the northern flank of the dome. Note tors in foreground and smoothness of dome surface.

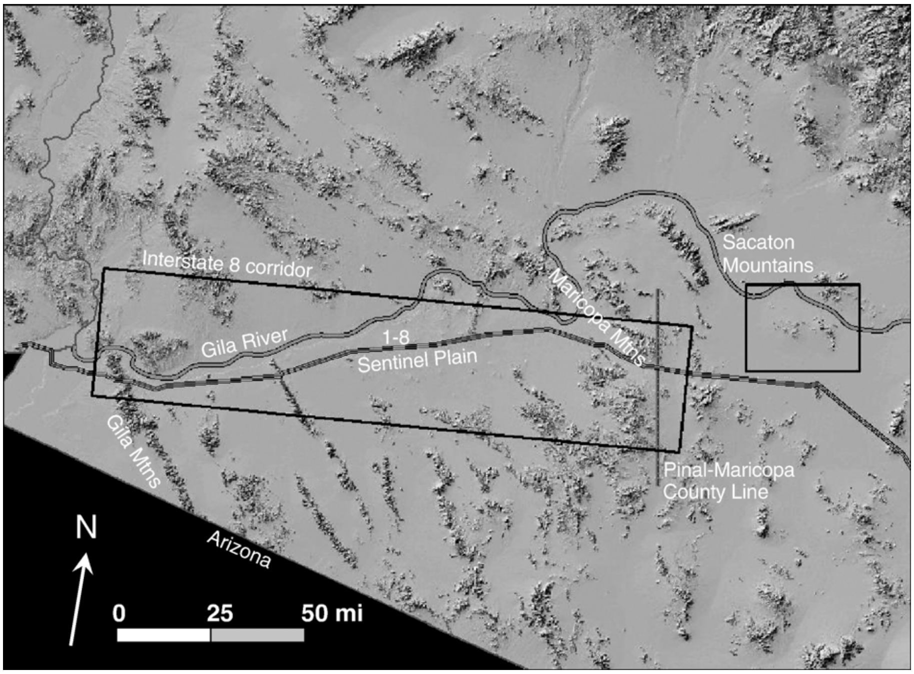

Fig. 8. Detailed location map for the surveyed Interstate 8 corridor, including a depiction of I-8 and the Gila River traversing southwestern Arizona. Pertinent political boundaries and geographic features noted.

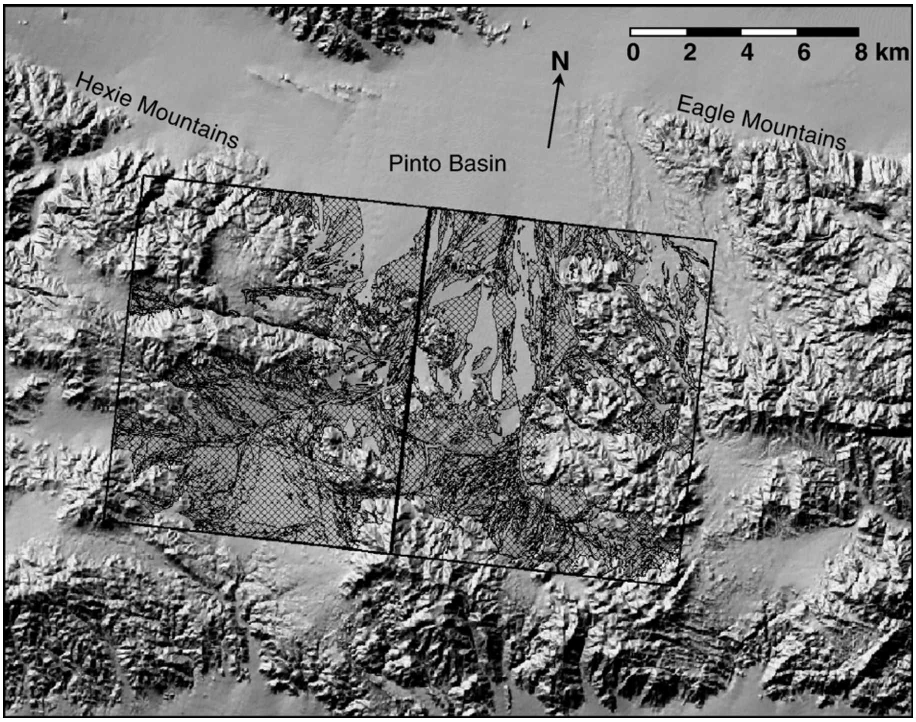

Fig. 9. Mapped pediment units (hatched regions) within Porcupine Wash (left) and Conejo Well (right) USGS 7.5′ geological quadrangle maps. Pinto Basin is hydrologically-open, and pediments fringe uplands as well as inhabit distal portions of basin, particularly in Conejo Well map.

and the Wonderland of Rocks) and exhibiting sharp slope discontinuities at their headward junction with upland mountain masses. Within our field area, spanning the Indian Cove, Queen Mountain, Keys View, Malapai Hill, and Fried Liver Wash 7.5′ USGS topographic quadrangles, Pleasant Valley provides the only hydrologically-closed boundary condition, although the basin feeding Wilson Canyon supports only two small peripheral washes, and distinctively lacks bedrock outcroppings or any form of channelization ornamenting its surface.

The Sacaton Mountains in the Sonora Desert of Arizona yield pediment surfaces that generally lack tors, and are composed of iron-stained gravels and cobbles of granitic and gneissic rocks heavily mantling bedrock surfaces (Bryan, 1922), although the regolith's thickness was not measured in the field. Pediment slopes range from approximately 0.5–3.0° (Bryan, 1922). Numerous desert washes on the mountains' southern flanks and the Gila River and Santa Cruz Wash to the north drain the pediment surfaces, creating hydrologically-open boundary conditions surrounding the entirety of the Sacaton Mountains.

We did not survey pediment surfaces along the I-8 corridor in detail, but pediments here generally exhibit poor drainage network integration, few, small channels draining surfaces coated with loose, grussy sediments, and occasional tors and inselbergs protruding through regolith mantles. All pediments here are locally hydrologically-open, although some Basin and Range topography ultimately traps runoff and sediments in playa basins beneath pediment-fringed, N–S trending ranges. It is no coincidence that I-8 penetrates and crosses these ranges at low elevation, low sloping pediment passes and domes (i.e., through the Mohawk Mountains; Fig. 8).

4.3. Results

Our field reconnaissance and previous work (Sharp, 1957) indicate that Cima Dome exhibits more widespread pedimentation extending across the dome's apex and to its south and southwest. The more extensive pediment surfaces to the southwest are associated with a subsidiary pediment dome, Cimacito Dome (Sharp, 1957). Pedimentation is more restricted to the north of

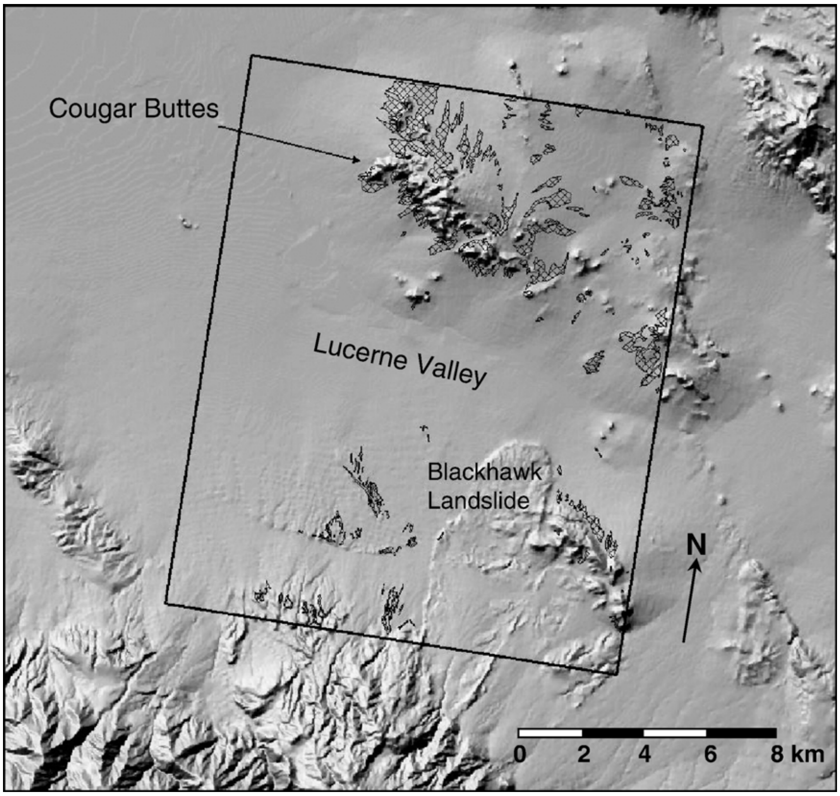

Fig. 10. Mapped pediment units (hatched regions) within Cougar Buttes USGS 7.5′ geological quadrangle map. Pediments fringe the Cougar Buttes and Blackhawk Mountain (south of landslide), and also appear partially buried by landslide deposit. Lucerne Valley is hydrologically-open locally, but feeds Lucerne Dry Lake off west side of image.

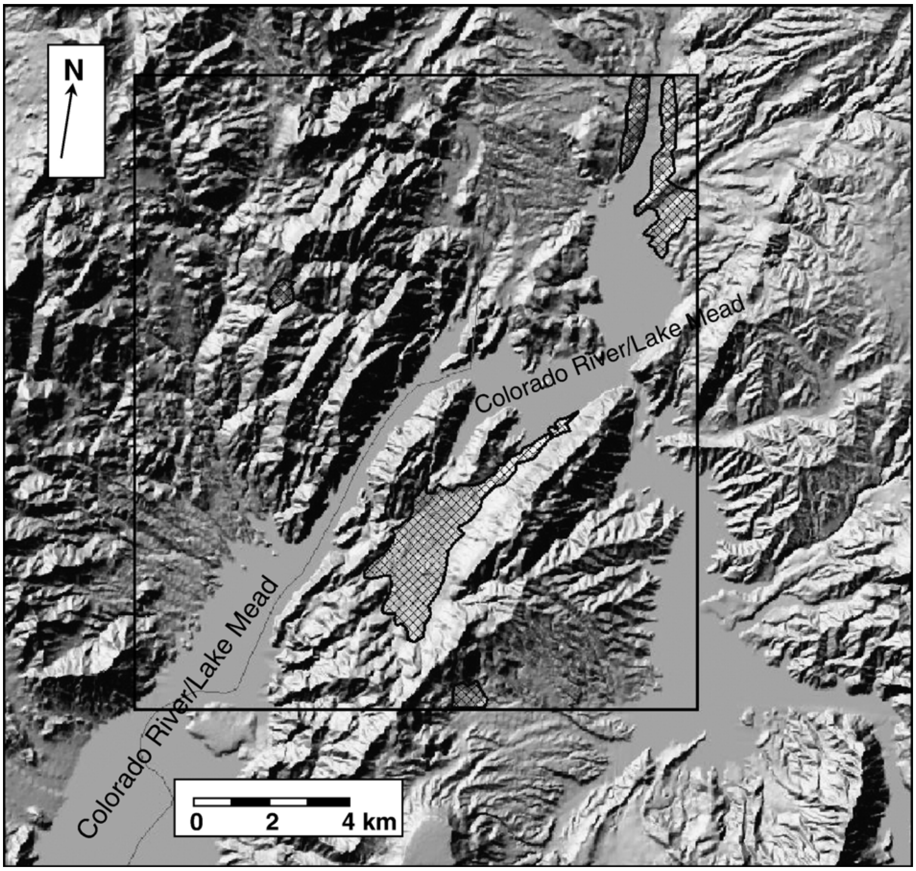

Fig. 11. Mapped pediment units (hatched regions) within Iceberg Canyon 7.5′ geological quadrangle map.

Cima Dome, with the exception of a small pediment pass extending northeast to Kessler Peak in the Ivanpah Mountains. The preferential extension of pediments to the south and southwest may be attributable to hydrologic boundary conditions during the development of the Cima Dome pediment: the Kelso–Cedar Wash drainage system to the south and southeast provide potential runoff and sediment removal, while drainage texture (Doering, 1970) and surface morphology in the Ivanpah and Shadow Valleys to the northeast and northwest, respectively, indicate hydrologically-closed drainage for the northern flanks of the dome. Additional support for restricted pedimentation with hydrologically-closed boundary conditions exists on the distal western portion of the dome where Cenozoic basaltic lava flows of the Cima Volcanic Field bury regolith profiles of at least 40 m thickness mantling Cretaceous granitic rocks (Dohrenwend et al., 1986). Tectonic warping (Sharp, 1957) or fault block tilting (Miller, 1995) may have complicated the nature of these boundary conditions, but current drainage form and texture supports predictions made by our model simulations.

The Granite Mountains do not in themselves provide a comparison of the effects of hydrologic boundary conditions on pedimentation because the piedmonts surrounding them are all well drained by desert washes. However, the extension of mantled, exhumed, and incised pediments to bounding desert washes is consistent with our modeling work predicting the presence of such geomorphic relations only in hydrologically-open basins. Additionally, we expect that these boundary conditions governed the geomorphic development of the Granite Mountains piedmont at least through the Pleistocene and Holocene because tors punctuating the full length of the pediment suggest base level incision (Strudley et al., 2006b) and because cosmogenic radionuclide-derived measurements of sediment transport rates across the Granite Mountains piedmont suggest a cessation of deposition in the late Pleistocene (Nichols et al., 2002).

The Sacaton Mountains in Arizona provide another example of a group of mountain residuals circumferentially bounded by hydrologically-open boundary conditions in the form of the Gila River and Santa Cruz Wash.

The Sacaton Mountains pediment extends across the length of the desert piedmont from piedmont junction to bounding channel while maintaining bare-bedrock edifices in the uplands, again, consistent with model results. Its morphology may signal an analogous, but earlier, stage in pediment dome evolution comparable to Cima Dome in the Mojave Desert.

Pediments in Joshua Tree National Park, including those mapped in the Conejo Well and Porcupine Wash geologic quadrangle maps (Fig. 9), support model predictions indicating a preferential development of pediments in hydrologically-open basins. Mountains flanking hydrologically-closed basins, such as Pleasant Valley and the upland basin feeding Wilson Canyon do not support pediments, while hydrologically-open basins support extensive pediment surfaces ornamented by tors and larger inselbergs.

The Cougar Buttes geologic quadrangle map indicates the presence of pediments preferentially on the northern flanks of the Cougar Buttes (Fig. 10), while the southern periphery of the Buttes obscures pediment surfaces with a coverage of various alluvial and colluvial surficial deposits (Cossette, 2000; Powell and Matti, 2000). Lucerne Dry Lake to the west forms a distally closed basin to which material derived from the Cougar Buttes ultimately collects, but desert washes in the headward portions of the Lucerne Valley appear to form hydrologically-open boundary conditions for pediment surfaces developing on the flanks of the Cougar Buttes. Tors and inselbergs protrude through sediment mantles near these desert washes. Thus, the distribution of pediment surfaces surrounding the Cougar Buttes again appears to be consistent with our model predictions concerning the influence of boundary conditions on pediment development.

Pediments in the Iceberg Canyon geologic quadrangle (Fig. 11), although predominantly carved on sedimentary rocks, also extend to hydrologically-open boundaries controlled by the Colorado River and surrounding mountain drainage systems (isolated pediment in east-central portion of map area, Fig. 11). It is unclear, however, what controls the specific placement of these pediment landforms, and why the Colorado River canyon within this area does not support the development of more pediment surfaces. Perhaps incision rates of the Colorado River at this location exceeded the integrated sediment flux derived from upslope weathering and sediment transport processes, precluding footslope pediment development.

Mountain ranges bisected by Interstate 8 in southwestern Arizona exhibit inconsistent relationships between the prevalence of footslope pediments and hydrologic boundary conditions. For example, drainage texture (Doering, 1970) and surface morphology in San Cristobal Valley and in the Mohawk Valley, which flank the pediment pass through which Interstate 8 traverses at the northern end of the Mohawk Mountains, suggests hydrologically-closed conditions, while the Gila River to the north of the range may provide an adequate means by which sediment may be removed from piedmont surfaces, creating a hydrologically-open boundary condition. Regardless of boundary condition, the presence of the pediment pass is consistent with model predictions indicating this type of landform as the ultimate state of a developing mountain front. Other field relations along the I-8 corridor complicate model testing: Sentinel Plain exhibits a pediment dome at Sentinel Peak, although the extent of this surface is unknown and the basalt flow upon which the Sentinel Plain is built exhibits a complex surface morphology that complicates local hydrologic boundary conditions. Also, the eastern flanks of the southern Maricopa Mountains, adjacent to Vekol Valley to the east, exhibit pediment surfaces, while the fringes of mountains fronts bordering the Bender Wash valley and the Interstate 8 corridor appear to lack pedimented surfaces. Last but not least, the Gila Mountains, closely bordered by the Gila River to the north, appear to lack pediments in favor of dissected alluvial fans. Model predictions may indeed be confirmed at this latter location if incision rates of the Gila River outpace the integrated sediment flux reaching the Gila River floodplain, leaving mountain slopes devoid of sediment except in local areas of temporary storage within dissected alluvial fans.

5. Discussion

Our model of pediment development provides testable predictions based on incorporation of the most pertinent geomorphological processes controlling piedmont evolution in many environments. However, our model omits certain processes that would complicate the morphology of geomorphic landforms our model can simulate, thus limiting its predictive capability in specific environments. For example, our model does not incorporate mass wasting processes, which in some locales may disrupt pedimentation on mountain footslopes. Our model would likely predict the presence of pediment surfaces, for example, at the foot of the Blackhawk Mountains, where Fig. 10 places the deposit left by the Blackhawk landslide. Interestingly, the geomorphic relations depicted in Fig. 10 may actually support our model's predictions if the small pediments mapped along the snout of the Blackhawk landslide deposit (Fig. 10) represent larger pediment landforms that were buried during their development.

Our model is also limited in its ability to simulate the full suite of weathering styles active in nature, particularly dissolution-style weathering that often characterizes limestone bedrock (Wilkinson and Humphreys, 2005). Although numerous workers identify pediments formed in limestones (see references in Introduction), subsurface dissolution of limestones underlying anticlinal structures north of the San Bernardino Mountains in southern California restrict the development of extensive equilibrium regolith profiles that characterize adjacent pediments built on granitic rocks (Eppes et al., 2002; Pearce et al., 2004). This limitation in the model's predictive capabilities is especially pertinent in areas underlain by alternating layers of clastic and chemical/biochemical rocks where controls on pedimentation may be a function of rock layer thickness and moisture regime.

Although our model seeks to elucidate climatic controls on pediment formation through simulations altering rainfall rate, soil hydrologic properties, sediment transport style, and subsurface weathering processes, our model does not explicitly model the effects and feedbacks between climate, vegetation, sediment transport, and bedrock weathering. For example, vegetation types and densities determine root growth and structure which can alter the plan form of fluvial channels (Murray and Paola, 2003), the development of biotic crusts and organic residues can alter soil hydrologic properties (Howes and Abrahams, 2003), and the development of organic acids and other molecules can potentially modulate bedrock weathering (Andrews and Schlesinger, 2001). Soil crusts may be particularly important in semi-arid environments, in which soil hydraulic conductivities may be less than in both arid and humid climates, thus drastically reducing infiltration capacity. The description and incorporation of probabilistic rainfall distribution characteristics (Eagleson, 1978; Hawk and Eagleson, 1992; Tucker and Bras, 2000) may also refine our hydrologic treatment, and we plan on incorporating an improved rainfall generation scheme in future modeling endeavors. We have also simplified our hydrologic balance by ignoring the effects of plant roots and stems on stemflow-derived infiltration and flow through macropores, evapotranspiration, and percolation and drainage through detritus in the O-horizon of soil. Our model does not simulate return flow, which may be important in some temperate and humid environments. However, all of these effects will become more important in more moist environments for which we have yet to test our model's predictive capabilities. In certain lithologic and climatic environments fluvial incision becomes important in preventing pedimentation by incising bedrock rather than leading to regolith thickness instability and tor growth. The omission of bedrock incision in our model reflects our initial observations illustrating its lack of importance on desert piedmonts; however, it is clear that its inclusion for simulating more humid environments with perennial streams would significantly alter the results presented in Fig. 5G–P. Further modeling and field work will be necessary to investigate the role that bedrock incision plays in modulating the development of pediment surfaces. Similarly, future modeling work will address pedimentation in light of the coupled effects between correlated weathering and hydrologic parameters (e.g., elevated d_1 coupled with higher rainfall rates and/or altered soil hydrologic properties in humid environments), although we would expect that this coupled test would yield similar results to their singular perturbations: a general lack of pediment formation in more humid environments.

Within the purview of our model's capabilities and the data available to test it with, described here, our model performs reasonably well in illustrating environments prone to pedimentation. However, the extent to which our test sites confirm our model predictions depends not only on the model's capabilities but also on the quality and interpretation of the field data. For example, local complications in tectonic and boundary conditions may explain why pediments are not more widespread in the Cougar Buttes and Iceberg Canyon geologic quadrangle maps. Based on the geomorphic and geologic descriptions provided by Powell and Matti (2000) for the Cougar Buttes quadrangle, we would classify many of the alluvial and colluvial map units as pediment regolith profiles (extending south from the Cougar Buttes to Lucerne Valley), which would enhance the success of our model's predictions. Well data and geophysical profiles would also aid in our discrimination of pediments from alluvial fans and basin deposits, improving our ability to test model predictions. Assessment of hydrologic boundary conditions, ascertained by visual inspection of field sites and satellite imagery, along with tectonic and lithologic variability associated with Basin and Range faulting and volcanism, may explain the model's predictive capability (or lack thereof) along the Interstate 8 corridor in southwestern Arizona.

In light of these limitations, we plan to expand our model testing endeavors by examining field sites for which detailed regolith thickness and boundary condition data constrained by well logs and tectonic and hydrologic investigations are available. Ancestral erosion surfaces exposed in the Big Bear Block of the San Bernardino Mountains in southern California and in the Rocky Flats/Boulder area of the Colorado Rockies provide candidate sites for which detailed tectonic investigations and well logs exist (Riley, 1956; John S. Murk Engineers, Inc. and LeRoy Crandall and Associates, 1985; Aksoy et al., 1986; Powell and Matti, 1998a, b; Spotila and Sieh, 2000; Knepper, 2003; Dethier and Lazarus, 2006). We invite other field site suggestions and the production of more extensive regolith thickness and mountain-front boundary condition data sets to supplement our model tests and to further constrain conditions in which pediments develop at the foot of growing or decaying mountains.

This study and previous modeling efforts describe pediments and their associated landforms (Strudley et al., 2006a,b) as dynamic, erosional landforms defined by the active development of a finite (~0–4 m) equilibrium regolith profile over bedrock forming smooth, unincised surfaces of low slope (0–10°). Here, we provide further modeling work that suggests an insensitivity of the pedimentation process to various lithologic configurations and climatic conditions. We therefore suggest that terms like peneplain, pediplain, pediplane, peri-pediment, rock fan, pan-fan, and other similarly confusing terms be removed from the geomorphologic vernacular in favor of one term, “pediment”, which may be modified by the adjectives “exhumed” (a pediment stripped of its regolith by a climatic or tectonic perturbation), “incised” (a pediment that has been corrugated locally by a deep drainage channel, and which is usually also exhumed), or “bare-bedrock” (pediments defined by an equilibrium regolith thickness that provides spatially sporadic or complete bedrock exposure). We would like to emphasize that the pediment landform consists of coupled bedrock and alluvial surfaces that lower together through time; the bedrock floor of the pediment is not the landform itself, because its origins are dictated by a feedback between bedrock weathering and regolith thickness, regardless of tectonic, climatic, or lithologic conditions. The terms “pediment dome” and “pediment pass” may be used to describe a pediment’s geomorphic position and/or maturity. We also suggest that erosional landforms, regardless of environment, characterized by a thin (~0–4 m) equilibrium regolith profile over extensive smooth surfaces be termed pediments such as the high alpine surfaces of the Wind River Range described by Anderson (2002). We advise the discrimination between strath terraces and pediments, the former of which have been misidentified as pediments (Wilshire and Reneau, 1992) because their morphology, reflecting floodplain deposition over beveled bedrock surfaces, mimics that of pediments, which are purely erosional landforms.

6. Conclusion

Here we describe the robust development of pediment landforms in a numerical modeling environment that incorporates a range of lithologic, climatic, and tectonic environments. Pediments develop at the foot of mountain slopes in environments characterized by 1) lithologies that weather into clastic debris; 2) climates that favor the development of soil hydrologic properties, plant communities, and weathering styles that suppress fluvial incision and deep bedrock weathering; and 3) hydrologically-open basin boundary conditions in which base level incision rates do not exceed the integrated sediment flux along the mountain slope. Pediments develop as pediment passes or domes with both hydrologically-open and -closed boundary conditions, although the latter boundary condition generally restricts the development of footslope pediments. Our model predictions are largely supported by a limited set of field observations and geologic data from the arid/semiarid southwestern United States that illustrate the prevalence of pediments in hydrologically-open basins and a lack of pediments in hydrologically-closed basins. The model simulations of pediment development in more humid environments await further field tests to ascertain the model’s predictive capabilities, but we expect that previously unrecognized pediments may exist in footslope positions in climatic regimes other than arid/semiarid as long as subsurface bedrock weathering is restricted as in arid environments. Model results suggest a ubiquity in the development of finite equilibrium regolith profiles in hydrologically-open basins, which suggests that the process of pedimentation may indeed be, as some early geomorphologists speculated, a general phenomenon common to developing and decaying mountain fronts around the world.

Acknowledgements

We extend special thanks to Peter K. Haff for the encouragement and the thought-provoking conversation that motivated this work. We also thank members of the Surface Processes Club at Duke University for discussions that stimulated this research. The United States Army Research Office [DAAD19-99-1-0191] and the Andrew W. Mellon Foundation provided partial support.

References

Aksoy, R., Sadler, P., Biehler, S., 1986. Granity anomalies over sedimentary basins on the Helendale fault trend. In: Kooser, M.A., Reynolds, R.E. (Eds.), Geology Around the Margins of the Eastern San Bernardino Mountains. Inland Geol. Soc., Redlands, CA, pp. 121–128.

Anderson, R.S., 2002. Modeling the tor-dotted crests, bedrock edges, and parabolic profiles of high alpine surfaces of the Wind River Range, Wyoming. Geomorphology 46, 35–58.

Andrews, J.A., Schlesinger, W.H., 2001. Soil CO_2 dynamics, acidification, and chemical weathering in a temperate forest with experimental CO_2 enrichment. Global Biogeochemical Cycles 15, 149–162.

Ballesteros, E.M., Martin, M.C., 2002. Study of weathering processes developed on old piedmont surfaces in Western Spain: new contributions to the interpretation of the "Rana" profiles. Geomorphology 42, 279–292.

Barth, H.K., 1976. Pedimentgenerationen und reliefentwicklung im schichstufenland Saudi-Arabiens. Zeitschrift fur Geomorphologie. Supplementband 24, 111–119.

Beauvais, A., Ritz, M., Parisot, J.-C., Bantsimba, C., 2003. Testing etching hypothesis for the shaping of granite dome structures beneath lateritic weathering landsurfaces using ERT method. Earth Surface Processes and Landforms 28, 1071–1080.

Bedient, P.B., Huber, W.C., 1992. Hydrology and Floodplain Analysis. Addison-Wesley Publishing Co., Reading, MA. 692 pp.

Berkey, C.P., Morris, F.K., 1932. Pediments in the Gobi. Bulletin of the Geological Society of America 43, 130.

Blackwelder, E., 1931. Desert plains. Journal of Geology 39, 133–140.

Boring, L. 1999. An empirical model of large scale sediment transport in arid terrain. M.S. Thesis, Duke University, Durham, 149 pp.

Bourne, J.A., Twidale, C.R., 1998. Pediments and alluvial fans: genesis and relationships in the western piedmont of the Flinders Ranges, South Australia. Australian Journal of Earth Sciences 45, 123–135.

Brady, R.J., Fryxell, J.E., Wernicke, B.P., 2002. Preliminary Geologic Map of the Iceberg Canyon Quadrangle, Clark County, Nevada and Mohave County, Arizona. Open-File Report 03-18. Nevada Bureau of Mines and Geology, Reno, NV.

Bryan, K., 1922. Erosion and Sedimentation in the Papago Country, vol. 730. U.S. Geological Survey.

Bryan, K., 1932. Pediments developed in basins with through drainage as illustrated by the Socorro area, New Mexico. Bulletin of the Geological Society of America 43, 1–128.

Bryan, K., McCann, F.T., 1936. Successive pediments and terraces of the upper Rio Puerco in New Mexico. Journal of Geology 44, 145–172.

Bull, W.B., 1977. The alluvial-fan environment. Progress in Physical Geography 1, 222–270.

Carson, M.A., Kirkby, M.J., 1972. Hillslope Form and Process. Cambridge Univ. Press, New York.

Clarke, M.L., Rendell, H.M., 2006. Process-form relationships in Southern Italian badlands: erosion rates and implications for landform evolution. Earth Surface Processes and Landforms 31, 15–29.

Cooke, R.U., 1970. Morphometric analysis of pediments and associated landforms in the western Mojave Desert, California. American Journal of Science 269, 26–38.

Cossette, P.M., 2000. Geologic map and digital database of the Cougar Buttes 7.5′ quadrangle, San Bernardino County, California. U. S. Dept. of the Interior; U. S. Geological Survey.

Cossette, P.M., 2001a. Geologic map and digital database of the Conejo Well 7.5 minute quadrangle, Riverside County, California. U.S. Dept. of the Interior; U.S. Geological Survey.

Cossette, P.M., 2001b. Geologic map and digitial database of the Porcupine Wash 7.5 minute quadrangle, Riverside County, California. U.S. Dept. of the Interior.

Cox, N.J., 1980. On the relationship between bedrock lowering and regolith thickness. Earth Surface Processes and Landforms 5, 271–274.

Daly, C., Neilson, R.P., Phillips, D.L., 1994. A statistical-topographic model for mapping climatological precipitation over mountainous terrain. Journal of Applied Meteorology 33, 140–158.

Dethier, D.P., Lazarus, E.D., 2006. Geomorphic inferences from regolith thickness, chemical denudation, and CRN erosion rates near the glacial limit, Boulder Creek catchment and vicinity, Colorado. Geomorphology 75, 384–399.

Dietrich, W.E., Bellugi, D.G., Sklar, L.S., Stock, J.D., Heimsath, A.M., Roering, J.J., 2003. Geomorphic transport laws for predicting landscape form and dynamics. In: Wilcock, P.R., Iverson, R.M. (Eds.), Prediction in Geomorphology. Geophysical Monograph, vol. 135. American Geophysical Union, Washington, D. C.

Doering, D.O., 1970. Discrimination of pediments and alluvial fans from topographic maps. Geological Society of America Bulletin 81, 3109–3116.

Dohrenwend, J.C., 1982. Tectonic control of pediment distribution in the Western Great Basin. GSA Abstracts with Programs 14, 161.

Dohrenwend, J.C., 1994. Pediments in arid environments. In: Abrahams, A.D., Parsons, A.J. (Eds.), Geomorphology of Desert Environments. Chapman and Hall, London, pp. 321–353.

Dohrenwend, J.C., Wells, S.G., McFadden, L.D., Turrin, B.D., 1986. Pediment dome evolution in the Eastern Mojave Desert, California. In: Gardiner, V. (Ed.), International Geomorphology 1986 Part II. John Wiley and Sons, Ltd., Chichester, pp. 1047–1062.

Dunne, T., Aubry, B.F., 1986. Evaluation of Horton's theory of sheetwash and rill erosion on the basis of field experiments. In: Abrahams, A.D. (Ed.), Hillslope Processes. Allen and Unwin, Boston, pp. 31–53.

Dunne, T., Leopold, L.B., 1978. Water in Environmental Planning. W. H. Freeman and Company, New York, N.Y. 818 pp.

Eagleson, P.S., 1978. Climate, soil, and vegetation, 2. The distribution of annual precipitation derived from observed storm sequences. Water Resources Research 14, 713–721.

Eggler, D.H., Larson, E.E., Bradley, W.C., 1969. Granites, grusses, and the Sherman Erosion Surface, southern Laramie Range, Colorado–Wyoming. American Journal of Science 267, 510–522.

Eppes, M.C., McFadden, L.D., Matti, J., Powell, R., 2002. Influence of soil development on the geomorphic evolution of landscapes: an example from the transverse ranges of California. Geology 30, 195–198.

Fairbridge, R.W., 1977. Note on bornhardt formation—the King–Twidale exchange. Zeitschrift fur Geomorphologie 21, 368.

Fernandes, N.F., Dietrich, W.E., 1997. Hillslope evolution by diffusive processes: the timescale of equilibrium adjustments. Water Resources Research 33, 1307–1318.

Furbish, D.J., Fagherazzi, S., 2001. Stability of creeping soil and implications for hillslope evolution. Water Resources Research 37, 2607–2618.

Gilbert, G.K., 1877. Report on the geology of the Henry Mountains. U.S. Geographical and Geological Survey of the Rocky Mountain Region. U.S. Department of the Interior, Washington, D.C.

Granger, D.E., Kirchner, J.W., Finkel, R., 1996. Spatially averaged long-term erosion rates measured from in situ produced cosmogenic nuclides in alluvial sediment. Journal of Geology 104, 249–257.

Granger, D.E., Riebe, C.S., Kirchner, J.W., Finkel, R., 2001. Modulation of erosion on steep granitic slopes by boulder armoring, as revealed by cosmogenic ^{26}Al and ^{10}Be. Earth and Planetary Science Letters 186, 269–281.

Hawk, K.L., Eagleson, P.S., 1992. Climatology of station storm rainfall in the continental United States: Parameters of the bartlett-lewis and poisson rectangular pulses models. Ralph M. Parsons Laboratory, Hydrology and Water Resources Systems, pp. 330.

Hanks, T.C., Bucknam, R.C., Lajoie, K.R., Wallace, R.E., 1984. Modification of wave-cut and fault-controlled landforms. Journal of Geophysical Research 89, 5771–5790.

Heimsath, A.M., Dietrich, W.E., Nishiizumi, K., Finkel, R.C., 1997. The soil production function and landscape equilibrium. Nature 388, 358–361.

Heimsath, A.M., Dietrich, W.E., Nishiizumi, K., Finkel, R.C., 1999. Cosmogenic nuclides, topography, and the spatial variation of soil depth. Geomorphology 27, 151–172.

Heimsath, A.M., Chappell, J., Dietrich, W.E., Nishiizumi, K., Finkel, R.C., 2000. Soil production on a retreating escarpment in southeastern Australia. Geology 28, 787–790.

Hirschberg, D.M., Pitts, G.S., 2000. Digital geologic map of Arizona: A digital database derived from the 1983 printing of the Wilson, Moore, and Cooper 1:500,000-scale map. Open-File Report 00-409, United State Dept. of the Interior; U.S. Geological Survey.

Howard, A.D., 1994. A detachment-limited model of drainage basin evolution. Water Resources Research 30, 2261–2285.

Howes, D.A., Abrahams, A.D., 2003. Modeling runoff and runon in a desert shrubland ecosystem, Jornada Basin, New Mexico. Geomorphology 53, 45–73.

John S. Murk Engineers, Inc., LeRoy Crandall and Associates, 1985. Historic and present conditions, upper Mojave River basin: Apple Valley, CA, Mojave Water Agency, Apple Valley, CA.

Jyotsna, R., Haff, P.K., 1997. Microtopography as an indicator of modern hillslope diffusivity in arid terrain. Geology 25, 695–698.

King, L.C., 1949. The pediment landform: some current problems. Geological Magazine 86, 245–250.

King, L.C., 1953. Canons of landscape evolution. Geological Society of America Bulletin 64, 721–752.

Knechtel, M.M., 1953. Pediments of the Little Rocky Mountains, North-Central Montana. Bulletin of the Geological Society of America 64, 1445.

Knepper Jr., D.H., 2003. Shapefile of the elevation of the bedrock surface beneath the Rocky Flats Alluvial Fan, Boulder and Jefferson Counties, Colorado. Open-File Report 03-443, U. S. Dept. of the Interior; U. S. Geological Survey.

Miller, V.C., 1948. Pediments and pediment-forming processes near House Rock, Arizona. Journal of Geology 58, 634–645.

Miller, D.M., 1995. Characteristics, age, and tectonic implications of the Mid Hills Pediment. SBCMA Quarterly 42, 69–74.

Miller, D.M., Miller, R.J., Nielson, J.E., Wilshire, H.G., Howard, K.A., Stone, P., 1991. Preliminary geologic map of the East Mojave National Scenic Area, California. Open-File Report 91-435. USGS.

Mills, H.H., 1983. Pediment evolution at Roan Mountain, North Carolina, USA. Geografiska Annaler. Series A. Physical Geography 65, 111–126.

Morris, F.K., 1932. Some pediments in Arizona. Bulletin of the Geological Society of America 43, 129.

Murray, A.B., Paola, C., 2003. Modelling the effect of vegetation on channel pattern in bedload rivers. Earth Surface Processes and Landforms 28, 131–143.

Nichols, K.K., Bierman, P.R., Hooke, R.L., Clapp, E.M., Caffee, M., 2002. Quantifying sediment transport on desert piedmonts using ^{10}Be and ^{26}Al. Geomorphology 45, 105–125.

Nichols, K.K., Bierman, P.R., Caffee, M., Finkel, R., Larsen, J., 2005. Cosmogenically enabled sediment budgeting. Geology 33, 133–136.

NOAA, 1999. Hourly Precipitation Data. National Oceanic and Atmospheric Administration, National Climatic Data Center, Ashville, NC.

Oberlander, T.M., 1972. Morphogenesis of granitic boulder slopes in the Mojave Desert, California. Journal of Geology 80, 1–20.

Oberlander, T.M., 1974. Landscape inheritance and the pediment problem in the Mojave Desert of Southern California. American Journal of Science 274, 849–875.

Pavich, M.J., 1989. Regolith residence time and the concept of surface age of the piedmont "peneplain". Geomorphology 2, 181–196.

Pearce, S.A., Pazzaglia, F.J., Eppes, M.C., 2004. Ephemeral stream response to growing folds. Geological Society of America Bulletin 116. doi:10.1130/B25386.1.

Powell, R., 2001a. Geologic map and digital database of the Conejo Well 7.5 minute quadrangle, Riverside County, California. Open-File Report 01-31, U. S. Dept. of the Interior; U. S. Geological Survey.

Powell, R., 2001b. Geologic map and digitial database of the Porcupine Wash 7.5 minute quadrangle, Riverside County, California. Open-File Report 01-30, U. S. Dept. of the Interior; U. S. Geological Survey.

Powell, R.E., Matti, J., 1998a. Stratigraphic and geomorphic relations between the Mojave Desert and San Bernardino Mts. piedmont, Lucerne Valley, CA: Part 1. The Geological Society of America 94th Annual Meeting: Cordilleran Section. Geological Society of America, CSULB Pyramid and Pointe Conference Center, Long Beach, CA, p. 59.

Powell, R.E., Matti, J., 1998b. Stratigraphic and geomorphic relations between the Mojave Desert and San Bernardino Mts. piedmont, Lucerne Valley, CA: Part 2. The Geological Society of America 94th Annual Meeting: Cordilleran Section. Geological Society of America, CSULB Pyramid and Pointe Conference Center, Long Beach, CA, p. 59.

Powell, R., Matti, J., 2000. Geologic map and digital database of the Cougar Buttes 7.5′ quadrangle, San Bernardino County, California. Summary Pamphlet: Late Cenozoic deposits of the Cougar Buttes 7.5′ quadrangle, San Bernardino County, California, U. S. Dept. of the Interior; U. S. Geological Survey.

Rich, J.L., 1935. Origin and evolution of rock fans and pediments. Geological Society of America Bulletin 46, 999–1024.

Riebe, C.S., Kirchner, J.W., Finkel, R., 2004. Erosional and climatic effects on long-term chemical weathering rates in granitic landscapes spanning diverse climatic regimes. Earth and Planetary Science Letters 224, 547–562.

Riley, F.S., 1956. Data on water wells in Lucerne, Johnson, Fry, and Means Valleys, San Bernardino County, California. Open File Report, U. S. Geological Survey and California Division of Water Resources, Long Beach, CA.

Ruxton, B.P., 1958. Weathering and subsurface erosion in granite at the piedmont angle, Balos, Sudan. Geological Magazine 95, 353–377.

Ruxton, B.P., Berry, L., 1961. Notes on faceted slopes, rock fans and domes on granite in the east-central Sudan. American Journal of Science 259, 194–206.

Schumm, S.A., 1962. Erosion on miniature pediments in Badlands National Monument, South Dakota. Geological Society of America Bulletin 73, 719–724.

Sharon, D., 1962. On the nature of hamadas in Israel. Zeitschrift fur Geomorphologie 5, 129–147.
Sharp, R.P., 1957. Geomorphology of Cima Dome, Mojave Desert, California. Geological Society of America Bulletin 68, 273–290.
Spotila, J.A., Sieh, K., 2000. Architecture of transpressional thrust faulting in the San Bernardino Mountains, southern California, from deformation of a deeply weathered surface. Tectonics 19, 589–615.
Stewart, J.H., Carlson, J.E., Raines, G.L., Connors, K.A., Moyer, L.A., Miller, R.J., 2003. Spatial digital database for the geologic map of Nevada. Open-File Report 03-66, U. S. Dept. of the Interior.
Strudley, M.W., Murray, A.B., Haff, P.K., 2006a. The emergence of pediments, tors, and piedmont junctions from a bedrock weathering-regolith thickness feedback. Geology 34, 805–808.
Strudley, M.W., Murray, A.B., Haff, P.K., 2006b. Regolith-thickness instability and the formation of tors in arid environments. Journal of Geophysical Research-Earth Surface 111. doi:10.1029/2005JF000405.
Tarboton, D.G., 1997. A new method for the determination of flow directions and upslope areas in grid digital elevation models. Water Resources Research 33, 309–319.
Thomas, M.F., 1965. Some aspects of the Geomorphology of domes and tors in Nigeria. Zeitschrift fur Geomorphologie 9, 63–81.
Thomas, M.F., 1989. The role of etch processes in landform development I. Etching concepts and their applications. Zeitschrift fur Geomorphologie 33, 129–142.
Tucker, G.E., Bras, R.L., 2000. A stochastic approach to modeling the role of rainfall variability in drainage basin evolution. Water Resources Research 36, 1953–1964.
Twidale, C.R., 1979. The character and interpretation of some pediment mantles. Sedimentary Geology 22, 1–20.
Twidale, C.R., 1981. Origins and environments of pediments. Journal of the Geological Society of Australia 28, 423–434.
Vanoni, V.A. (Ed.), 1975. Sedimentation Engineering. ASCE Manuals and Reports on Engineering Practice-No. 54. American Society of Civil Engineers, New York. 745 pp.
Vincent, P., Sadah, A., 1996. The profile form of rock-cut pediments in western Saudi Arabia. Journal of Arid Environments 32, 121–139.
Wahrhaftig, C., 1965. Stepped topography of the Southern Sierra Nevada, California. Geological Society of America Bulletin 76, 1165–1190.
Warnke, D.A., 1969. Pediment evolution in the Halloran Hills, central Mojave Desert, California. Zeitschrift fur Geomorphologie 13, 357–389.
Whitaker, C.R., 1979. The use of the term 'pediment' and related terminology. Zeitschrift fur Geomorphologie 23, 427–439.
Wilkinson, M.T., Humphreys, G.S., 2005. Exploring pedogenesis via nuclide-based soil production rates and OSL-based bioturbation rates. Australian Journal of Soil Research 43, 767–779.
Wilkinson, M.T., Chappell, J., Humphreys, G.S., Fifield, K., Smith, B., Hesse, P., 2005. Soil production in heath and forest, Blue Mountains, Australia: influence of lithology and palaeoclimate. Earth Surface Processes and Landforms 30, 923–934.
Wilshire, H.G., Reneau, S.L., 1992. Geomorphic surfaces and underlying deposits of the Mohave Mountains Piedmont, Lower Colorado River, Arizona. Zeitschrift fur Geomorphologie 36, 207–226.